

Inertial effects on the interphase drag force and rheology of dilute suspensions of buoyant droplets at low Reynolds number

Nicolas Fintzi and Jean-Lou Pierson

January 28, 2026

Abstract

In this work, we compute the hydrodynamic force and the first and second moments of force acting on a translating spherical droplet immersed in a uniform flow using the reciprocal theorem. We consider the low but finite Reynolds number regime, $Re = aU\rho_f/\mu_f$, and the dilute limit of small droplet volume fraction ϕ . Here, U denotes the magnitude of the relative velocity between the phases, a the droplet radius, and ρ_f and μ_f the density and viscosity of the continuous phase, respectively. We show that the $O(Re)$ inertial corrections to the first and second moments of force scale as $O(\rho_f\phi U^2)$ and $O(a\rho_f\phi U^2)$, respectively. Moreover, the ensemble average of the drag force and the higher-order force moments over the distribution of droplet velocities introduces additional contributions proportional to the velocity variance of the dispersed phase, both in the interphase momentum exchange and in the effective stress of the continuous phase. As a consequence, in dilute emulsions of buoyant droplets, the effective stress depends quadratically on the relative velocity between the phases, on the velocity variance of the dispersed phase, and on the spatial gradients of these quantities.

1 Introduction

Dispersed two-phase flows composed of droplets or bubbles are ubiquitous in processes developed at IFP Energies Nouvelles. Separation processes such as flotation rely on the injection of small bubbles to recover contaminants or dispersed droplets (Nguyen and Schulze, 2003). Dispersed phases are also widely used to enhance mass transfer, for instance in bubble columns (Kantarci et al., 2005) and liquid-liquid extractors (Weatherley, 2020), which can take various forms, including mixer-settlers and agitated columns. In all these processes, the flow is both turbulent and buoyancy-driven. Buoyancy plays an important role in separating the dispersed phase from the continuous phase. When buoyancy effects are too small, operational issues may arise, such as flooding in liquid-liquid extraction columns or the need for excessively large tanks in flotation systems. It is therefore essential to accurately predict the effects of relative motion between the phases in order to better design and optimize these processes.

At the process scale (typically on the order of meters), engineers cannot rely on direct numerical simulations, as their computational cost far exceeds the capabilities of current supercomputers and is incompatible with engineering timescales. Instead, modeling efforts rely on averaged equations of motion, which have proven accurate in predicting many two-phase flow phenomena. Even the simplest two-fluid models provide valuable insights into various aspects of two-phase flows, including the prediction of flooding in liquid-liquid extraction columns (Wallis, 2020). Since the work of Wallis (2020) and references therein, numerous refinements of two-fluid models have been proposed (Buyevich and Shchelchkova, 1979; Drew, 1983; Lhuillier, 1992; Zhang and Prosperetti, 1994; Jackson, 1997). Because the present study focuses on dispersed two-phase flows, we adopt the hybrid formalism originally developed by Buyevich and Shchelchkova (1979); Lhuillier (1992); Zhang and Prosperetti (1994); Jackson (1997). This formalism enables the derivation of physically grounded closure laws for both the continuous and dispersed phases. However, even for dilute buoyancy dominated flows, only a limited number of closure models are currently available in the literature, motivating the present work. Most previous studies on dilute suspensions have focused either on the Stokes flow regime or on the potential flow limit, and have examined how momentum exchange terms in two-fluid equations —namely, the drag force and higher-order moments of the hydrodynamic forces— affect the behaviour of the two phases.

The drag force acting on a droplet immersed in a uniform, steady Stokes flow was first derived by Hadamard (1911) and Rybczynski (1911). Its extension to steady but non-uniform flows, commonly referred to as the Faxén correction, was obtained by Het-sroni and Haber (1970) (see also Zhang and Prosperetti (1997) and Fintzi and Pierson (2025) for derivations within a two-fluid framework). Einstein (Einstein, 1905) was the first to show that the effective viscosity of a dilute suspension of solid spheres immersed in a viscous fluid is increased. This result was later extended by Taylor (1932) to suspensions of spherical droplets, demonstrating that the viscosity increase depends on the viscosity ratio between the phases. At the time, the connection between suspension viscosity and the first moment of the hydrodynamic force —whose deviatoric part for a solid particle is now known as the stresslet— had not yet been established. This link was later clarified by Batchelor (1970), who showed that the averaged symmetric part of the first force moment accounts for the increase in effective viscosity. It is worth noting that a spherical inclusion translating in a uniform flow does not generate a stresslet, which vanishes in this configuration. Subsequently, Lhuillier (1996), Jackson (1997), and Zhang and Prosperetti (1997), still within the framework of viscous and dilute suspensions, demonstrated that the second moment of the hydrodynamic force also contributes to the suspension rheology, leading to non-Newtonian behaviour. Because the second force moment appears under a divergence operator in the effective stress, it induces a non-homogeneous rheology. As a result, such suspensions may also be described as second-gradient fluids (Gatignol, 2023). Higher-order force moments were computed by Zhou and Prosperetti (2020), although their relevance in practical two-fluid models remains questionable, since their magnitude decreases rapidly with increasing order under the assumption of scale separation (Jackson, 1997; Fintzi and Pierson, 2025).

In the opposite limit of potential flow, several studies have investigated momentum transfer between the two phases. It is well known that the force acting on a spherical particle immersed in a uniform inviscid potential flow reduces to the added-mass force

(Pozrikidis, 2011). The dissipation method originally developed by Levich (Levich, 1962) allows to determine the drag force on a steadily moving bubble by considering a kinetic-energy budget over the entire fluid domain. Biesheuvel and Van Wijngaarden (1984) computed both the force and the first moment for a dilute suspension of translating spherical bubbles in potential flow, and additionally derived the Reynolds stresses induced by bubble motion. This contrasts with the Stokes-flow regime, in which the slow decay of the disturbance fields generated by particle motion leads to divergent integrals for the Reynolds stresses (Caflisch and Luke, 1985; Fintzi, 2025). At the same time, Ryskin and Rallison (1980), using an extension of Levich dissipation method, derived the increase in suspension viscosity due to bubbles immersed in a purely extensional flow at very high Reynolds numbers. Later, Zhang and Prosperetti (1994), within the hybrid formalism, extended the work of Biesheuvel and Van Wijngaarden (1984) by accounting for a finite variance of the particle centre-of-mass velocity. In parallel, several authors focused on closures for the dispersed-phase equations, including particle velocity fluctuations and collisional contributions (Sangani and Didwania, 1993; Bulthuis et al., 1995).

A large number of results are available in the literature for the force and torque acting on a spherical particle immersed in a flow at low but finite Reynolds number (see Leal (1980), Candelier et al. (2023), and references therein). In contrast, still within the low but finite Reynolds-number regime, very few results exist for higher-order moments of the hydrodynamic force. Notable exceptions are the studies of Lin et al. (1970), Stone et al. (2001), and later Raja et al. (2010), who investigated the small effects of fluid inertia on suspensions of neutrally buoyant spheres or droplets, respectively, immersed in viscous linear flows. These authors computed the first inertial correction to the first moment of the hydrodynamic force (Lin et al., 1970), as well as the pseudo-turbulent stress (Stone et al., 2001; Raja et al., 2010). In this framework, the resulting mixture can be assimilated to a Reiner-Rivlin fluid, since the effective stress was found to be proportional to the square of the mean shear rate in the steady-state regime. It is worth noting, however, that the closures proposed in these works are not material-frame indifferent, a limitation that is still the subject of discussion in the modeling of inertial suspension (Ryskin and Rallison, 1980).

The originality of this work lies in our focus on buoyant droplets translating at low but finite Reynolds number, a configuration that has not previously been investigated within the framework of averaged two-phase flow equations. We compute both the first and second moments of the hydrodynamic force, thereby including rheological contributions to the effective stress of a buoyant suspension. A second contribution of this study is the formulation of a general reciprocal relation that enables the computation of all force moments acting on droplets, including the drag force and the first and second moments. In this respect, the methodology adopted here is closely related to that employed in Stone et al. (2001), and Raja et al. (2010). Finally, by adopting a rigorous statistical averaging procedure, we show explicitly how velocity-variance terms arise in the ensemble-averaged drag force and in the effective stress of the continuous phase. It should be noted, however, that the system of equations is not fully closed, as no explicit closure is proposed for the velocity-variance terms appearing in the averaged momentum equations. Although some hints on their modelling are provided in Fintzi and Pierson (2025).

This manuscript is organized as follows. In Section 2.1 we recall the averaged mass

and momentum equations, and identify the terms that require closure relations. We then show in [Section 2.2](#) how the moments of hydrodynamic forces are related to conditionally averaged fields, which are governed by the conditionally averaged equations presented in [Section 2.3](#). To avoid the complete resolution of these equations, we derive in [Section 3](#) a general reciprocal relation. This relation provides a systematic method for computing force moments of arbitrary order acting on a droplet. Then, in [Section 4](#) we compute the $O(Re)$ corrections to the force moments acting on a droplet immersed in a uniform flow. These moments are then ensemble-averaged in [Section 5](#). Finally, in [Section 6](#) all results are incorporated into the averaged equations introduced in [Section 2.1](#) and discuss the rheological behaviors of the suspension.

2 Problem formulation

2.1 Averaged equations for dispersed two-phase flows

To clarify the respective roles of forces and higher-order moments in dispersed two-phase flow modeling, we first introduce the averaged mass and momentum equations for the dispersed and continuous phases, obtained through an ensemble-averaging procedure. For a monodisperse suspension, the governing mass and momentum equations for each phase can be expressed as ([Fintzi and Pierson, 2025](#))

$$\phi_f + \phi \approx 1, \quad (2.1)$$

$$\nabla \cdot \mathbf{U} = 0, \quad (2.2)$$

$$(\partial_t + \mathbf{U}_p \cdot \nabla) \phi = -\phi \nabla \cdot \mathbf{U}_p, \quad (2.3)$$

$$\rho_p \phi (\partial_t + \mathbf{U}_p \cdot \nabla) \mathbf{U}_p = \phi (\nabla \cdot \boldsymbol{\Sigma} + \rho_p \mathbf{g}) + \nabla \cdot \boldsymbol{\Sigma}_p^{\text{eff}} + \mathbf{F}, \quad (2.4)$$

$$\rho_f \phi_f (\partial_t + \mathbf{U}_f \cdot \nabla) \mathbf{U}_f = \phi_f (\nabla \cdot \boldsymbol{\Sigma} + \rho_f \mathbf{g}) + \nabla \cdot \boldsymbol{\Sigma}_f^{\text{eff}} - \mathbf{F}, \quad (2.5)$$

respectively. Note that in contrast to ([Fintzi and Pierson, 2025](#)), all ensemble averaged quantities are written using capital letters. The subscripts f and p refer to the continuous phase and the dispersed phase, respectively. The vector \mathbf{g} is the acceleration of gravity, ρ_k is the density, μ_k is the viscosity, and \mathbf{U}_k is the averaged velocity of phase k . We use the notation $\phi = n_p v_p$, where n_p is the droplet number density and v_p is the volume of a single droplet. ϕ_f is the volume fraction of the continuous phase. $\boldsymbol{\Sigma} = -P_f \boldsymbol{\delta} + 2\mu_f \mathbf{E}$, with $\mathbf{E} = \frac{1}{2}[\nabla \mathbf{U} + (\nabla \mathbf{U})^\dagger]$, is the *mean Newtonian stress* of the mixture, with P_f being the mean hydrodynamic pressure, and $\mathbf{U} = \phi_f \mathbf{U}_f + \phi \mathbf{U}_p$ the averaged velocity of the mixture¹, $\boldsymbol{\Sigma}_p^{\text{eff}}$ and $\boldsymbol{\Sigma}_f^{\text{eff}}$ are the effective stresses of the dispersed and continuous phase, respectively. Finally, \mathbf{F} represents the interphase momentum exchange.

The number density, continuous phase volume fraction, interphase force, and effective stresses of the dispersed and continuous phase can be expressed formally as ([Fintzi](#)

¹Note that the definition of ϕ and \mathbf{U} are only exact in the homogeneous regime ([Fintzi and Pierson, 2025](#)).

and Pierson, 2025),

$$n_p = \langle \delta_p \rangle, \quad (2.6)$$

$$\phi_f = \langle \chi_f \rangle, \quad (2.7)$$

$$\mathbf{F} = \left\langle \delta_p \oint_{\Gamma_\alpha} \boldsymbol{\sigma}_f^* \cdot \mathbf{n} d\Gamma \right\rangle, \quad (2.8)$$

$$\boldsymbol{\Sigma}_p^{\text{eff}} = -\langle \delta_p \mathbf{u}'_\alpha \mathbf{u}'_\alpha \rangle, \quad (2.9)$$

$$\begin{aligned} \boldsymbol{\Sigma}_f^{\text{eff}} = & -\langle \chi_f \rho_f \mathbf{u}'_f \mathbf{u}'_f \rangle + \left\langle \delta_p \oint_{\Gamma_\alpha} \mathbf{r} \boldsymbol{\sigma}_f^* \cdot \mathbf{n} d\Gamma - \delta_p \int_{\Omega_\alpha} 2\mu_f \mathbf{e}_d^* d\Omega \right\rangle \\ & - \nabla \cdot \left\langle \delta_p \frac{1}{2} \oint_{\Gamma_\alpha} \mathbf{r} \mathbf{r} \boldsymbol{\sigma}_f^* \cdot \mathbf{n} d\Gamma - \delta_p \int_{\Omega_\alpha} 2\mu_f \mathbf{r} \mathbf{e}_d^* d\Omega \right\rangle + \nabla \nabla (\dots). \end{aligned} \quad (2.10)$$

respectively. Here the operator $\langle \dots \rangle$ denotes ensemble averaging, χ_f is the phase indicator function of the continuous phase, $\delta_p = \sum_\alpha \delta(\mathbf{x} - \mathbf{x}_\alpha)$ is the distribution pointing on the particles centre of mass (denoted \mathbf{x}_α), and \mathbf{n} the unit vector normal (outward) to the droplets surface. \mathbf{u}_α is the centre of mass velocity of a particle labelled α . Ω_α and Γ_α , represent the volume and surface, respectively, of the droplets α . The superscript ' indicates the relative values of a quantity with respect to its phase- or particle-averaged value. Specifically, $p'_f = p_f^0 - P_f$, $\mathbf{u}'_\alpha = \mathbf{u}_\alpha - \mathbf{U}_p$, and $\mathbf{u}'_f = \mathbf{u}_f^0 - \mathbf{U}_f$, with \mathbf{u}_f^0 and p_f^0 , the local (non-averaged) velocity and pressure fields of the continuous phase. The superscript * represents the relative values of a quantity with respect to the mixture ensemble averaged value, such that $\boldsymbol{\sigma}_f^* = \boldsymbol{\sigma}_f^0 - \boldsymbol{\Sigma}$ and $\mathbf{e}_d^* = \mathbf{e}_d^0 - \mathbf{E}$, where $\boldsymbol{\sigma}_f = -p_f^0 + \mu_f [\nabla \mathbf{u}_f^0 + (\nabla \mathbf{u}_f^0)^\dagger]$ is the local stress of the continuous phase, and $\mathbf{e}_d^0 = \frac{1}{2} (\nabla \mathbf{u}_d^0 + \nabla \mathbf{u}_d^0)^\dagger$, is the internal shear rate within the droplet phase. Note that \mathbf{u}_d^0 is the internal velocity field of the fluid within the droplets, in opposition to \mathbf{u}_α which is the centre of mass velocity.

In this work, our focus is specifically on \mathbf{F} and on the second and third contributions appearing in the effective stress tensor $\boldsymbol{\Sigma}_f^{\text{eff}}$.

2.2 The closure problem

In the present context, the closure problem consists in expressing all ensemble-averaged terms of the form $\langle \dots \rangle$ in Eqs. (2.8) to (2.10) solely in terms of the macroscopic variables namely n_p , ϕ_f , P_f , \mathbf{U}_p , and \mathbf{U}_f . We now assume that the droplets are spherical with radius a . The surface exchange terms may be rewritten in terms of integrals of conditional averaged quantities (Lhuillier, 1992; Zhang and Prosperetti, 1997; Fintzi, 2025). If we take the example of the drag force term, we obtain,

$$\left\langle \delta_p \oint_{\Gamma_\alpha} \boldsymbol{\sigma}_f^* \cdot \mathbf{n} d\Gamma \right\rangle = \int_{\mathbb{R}^3} P[\mathbf{w}|\mathbf{x}, t] n_p[\mathbf{x}, t] \oint_{\Gamma_p} \{p_f^1 \boldsymbol{\delta} + \mu_f [\nabla \mathbf{u}^1 + \nabla \mathbf{u}^1]^\dagger\} \cdot \mathbf{n} d\Gamma(\mathbf{r}) d^3 \mathbf{w}, \quad (2.11)$$

where $p_f^1[\mathbf{r}|\mathbf{x}, \mathbf{w}]$ and $\mathbf{u}^1[\mathbf{r}|\mathbf{x}, \mathbf{w}]$, are the pressure and velocity fields ensemble averaged on every configuration where a droplet is located at \mathbf{x} with centre of mass velocity \mathbf{w} , minus the ensemble averaged pressure and velocity fields, i.e. $P_f[\mathbf{r}, t]$, and $\mathbf{U}[\mathbf{r}, t]$, \mathbf{r} being the points on the droplets surface. Γ_p denotes the surface of the test droplet whose surface may be expressed as $|\mathbf{x} - \mathbf{y}| = \mathbf{r} = a$. Here, $P[\mathbf{w}|\mathbf{x}, t]$ is the probability of

finding a droplet with centre of mass velocity \mathbf{w} knowing that a droplet is present at \mathbf{x} at time t . The equations governing p_f^1 and \mathbf{u}^1 can be obtained by conditionally averaging the local mass and momentum equations (Fintzi, 2025). The kinematics boundary conditions at the interface of the test droplet are well-defined only if the conditional average is performed on a sample of configurations where the droplets posses the same centre of mass velocity and shape. Hence, conditionally averaging on the centre of mass position \mathbf{x} , and on the centre of mass velocity \mathbf{w} , is a necessary step to reduce the degree of freedom of the conditionally averaged problem.

In the following, we consider arbitrary values of density and viscosity ratios, defined as:

$$\lambda = \mu_p / \mu_f, \quad \zeta = \rho_p / \rho_f, \quad (2.12)$$

respectively. Additionally, we limit this theoretical investigation to dilute suspensions ($\phi \ll 1$). We defined the droplet Reynolds number as,

$$Re = \frac{U \rho_f a}{\mu_f}, \quad (2.13)$$

where a is the radius of the droplets, and $U = |\mathbf{w}_r[\mathbf{y}]|$, with $\mathbf{w}_r[\mathbf{x}] = \mathbf{U}[\mathbf{x}] - \mathbf{w}$, the magnitude of the relative velocity between the centre of mass velocity of the test droplet and the ensemble averaged velocity of the mixture evaluated at the centre of mass position \mathbf{y} . Note that the value of the Reynolds number is considered arbitrary up to Section 4.2 where we consider a small but finite Reynolds number. Finally, the *capillary* number,

$$Ca = \mu_f U / \gamma, \quad (2.14)$$

is assumed to be small enough so that the droplets remain spherical.

2.3 Conditionally averaged equations

At the leading order in droplet volume fraction, the governing equations for \mathbf{u}^1 and p_f^1 are equivalent to those of an isolated droplet immersed in an unbounded domain (Hinch, 1977; Koch, 1993). Hence, we consider the problem of an isolated test droplet immersed in an arbitrary flow where only the uniform relative motions induce inertia. The disturbances pressure and velocity fields (\mathbf{u}^1 and p_f^1), relative to the position of a test droplet are noted \mathbf{u}_o , \mathbf{u}_i , p_o and p_i , for the velocity outside, and inside, the pressure outside, and inside the volume of the test droplet, respectively. Fig. 1 displays a schematic representation of the problem.

Outside and inside the volume of the test droplet we can write the mass and momentum equations for the disturbances fields ($p_{o/i}$ and $\mathbf{u}_{o/i}$) by conditionally averaging the Navier stokes equations (Koch, 1993; Fintzi, 2025). This lead to the equations for the disturbances fields originally derived by Maxey and Riley (1983) and Gatignol (1983). However, it is important to emphasize that-even in dilute suspensions-conditional averaging introduces additional contributions in Eqs. (2.16) and (2.18) (see (Koch, 1993, Eq. (9)) or Fintzi (2025)), which are not present in Maxey and Riley (1983) and Gatignol (1983)'s equations. In particular, one extra term corresponds to the velocity-variance of the conditionally averaged velocity field (see Koch (1993) or Fintzi (2025, Chapter 4)). In dilute flow, this term turns out to be negligible (Koch, 1993, Appendix A).

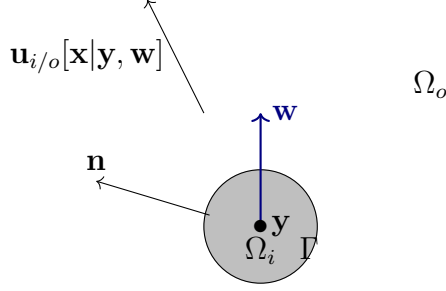


Figure 1: Sketch of the problem. $\mathbf{u}_{i/o}[\mathbf{x}|\mathbf{y}, \mathbf{w}]$ is the disturbance velocity field evaluated at \mathbf{x} , generated by a test droplet positioned at \mathbf{y} with centre of mass velocity \mathbf{w} . \mathbf{n} is the surface normal (outward) vector of the droplet. The exterior domain of the test droplet is denoted Ω_o , and the interior domain Ω_i .

Consequently, in the present context, we consider that the conditionally averaged equations are equivalent to the equations for an isolated droplet. The only difference is that conditionally averaged equations are explicitly related to ensemble-averaged fields (\mathbf{U} and P_f) through their boundary conditions (Fintzi, 2025). In dimensionless form, they read,

$$\nabla \cdot \mathbf{u}_o = 0 \quad (2.15)$$

$$\begin{aligned} \nabla \cdot \boldsymbol{\sigma}_o &= Re[\partial_t \mathbf{u}_o + \mathbf{u}_o \cdot \nabla \mathbf{u}_o + \mathbf{u}_o \cdot \nabla \mathbf{w}_r + \mathbf{w}_r \cdot \nabla \mathbf{u}_o] \\ &= Re \mathbf{f}_o, \end{aligned} \quad (2.16)$$

for all $|\mathbf{x} - \mathbf{y}| = |\mathbf{r}| = r > 1$, and,

$$\nabla \cdot \mathbf{u}_i = 0, \quad (2.17)$$

$$\begin{aligned} \nabla \cdot \boldsymbol{\sigma}_i &= (\zeta/\lambda - 1) \nabla \cdot \boldsymbol{\Sigma} + \frac{\zeta Re}{\lambda} [\partial_t \mathbf{u}_i + \mathbf{u}_i \cdot \nabla \mathbf{u}_i + \mathbf{u}_i \cdot \nabla \mathbf{w}_r + \mathbf{w}_r \cdot \nabla \mathbf{u}_i] \\ &= (\zeta/\lambda - 1) \nabla \cdot \boldsymbol{\Sigma} + \frac{\zeta}{\lambda} Re \mathbf{f}_i = \mathbf{f}_i^{\text{tot}}, \end{aligned} \quad (2.18)$$

for $r < 1$. The terms $\mathbf{f}_{o/i}$ denote dimensionless effective body force incorporating the inertial terms from the Navier-Stokes equations. Additionally, $\boldsymbol{\sigma}_{i/o} = -p_{i/o} \boldsymbol{\delta} + 2\mathbf{e}_{i/o}$ with $\mathbf{e}_{i/o} = \frac{1}{2} [\nabla \mathbf{u}_{i/o} + \nabla \mathbf{u}_{i/o}^{\dagger}]$ is the dimensionless Newtonian stresses in the interior and exterior of the test droplet. Note that the distances have been made dimensionless using the radius a , and the velocities using the velocity scale U . Likewise, the stresses in the exterior of the test droplet, and the ensemble averaged stress $\boldsymbol{\Sigma}$, have been made dimensionless using the viscous scale $U \mu_f/a$, and the stress in the interior of the test droplet using the scale $U \mu_d/a$. Because of the difference in viscosity and density between the dispersed and continuous phase $\mathbf{f}_i^{\text{tot}}$ includes in addition the divergence of the ensemble-averaged stress times the ratio of the material properties: $(\lambda/\zeta - 1)$. Note that in Eqs. (2.16) and (2.18), and in the following \mathbf{w}_r , \mathbf{U} and \mathbf{E} are dimensionless. In particular they correspond to $\mathbf{w}_r/U, \mathbf{U}/U$ and \mathbf{E}/U , respectively.

At the surface of the droplet ($r = 1$) the continuity of velocity and the non-deformability of the test droplet ($Ca \ll 1$), and the imposed velocity of the test droplet centre of mass, imposes,

$$\mathbf{u}_i - \mathbf{u}_o = 0, \quad (\mathbf{u}_i + \mathbf{w}_r) \cdot \mathbf{n} = 0. \quad (2.19)$$

$\mathbf{u}_i + \mathbf{w}_r$ can be interpreted as the velocity observed in the reference frame moving with the test droplet. The correct boundary condition for the disturbance shear rate is (at $r = 1$),

$$\mathbf{n} \cdot 2[\mathbf{e}_o - \lambda \mathbf{e}_i + (1 - \lambda) \mathbf{E}] \cdot (\boldsymbol{\delta} - \mathbf{n}\mathbf{n}) = \mathbf{b} \cdot (\boldsymbol{\delta} - \mathbf{n}\mathbf{n}), \quad (2.20)$$

with, $\mathbf{b}[\mathbf{r}, t]$ a tangential stress jump at the interface normalized by $\mu_f U/a$. Here we have considered a stress jump in order to stay general when deriving the reciprocal relation (see [Section 3](#)), nevertheless, \mathbf{b} will be taken to be zero in the final calculation of the moments of forces ([Section 4](#)). In particular, the contribution of Marangoni stresses to the rheology of the droplet suspension is not included in the present analysis (see [Fintzi and Pierson \(2025\)](#) for further discussion). Note that in general the ensemble averaged quantities \mathbf{U} and \mathbf{E} as well as \mathbf{b} depend on the position along the surface of the test droplet and time, so that $\mathbf{w}_r[\mathbf{r}, t]$, $\mathbf{E}[\mathbf{r}, t]$ and $\mathbf{b}[\mathbf{r}, t]$ in [Eqs. \(2.19\)](#) and [\(2.20\)](#) are not spatially constant. Hence, it is important to note that although $\mathbf{w}_r[\mathbf{y}]$ is a unit vector, $\mathbf{w}_r[\mathbf{x}]$ is not, because in the general case $\mathbf{U}[\mathbf{x}] \neq \mathbf{U}[\mathbf{y}]$.

For sufficiently large $|\mathbf{y} - \mathbf{x}|$, it is assumed that the conditionally averaged velocity and pressure fields are not affected by the presence of the test droplet, hence they are equal to their respective ensemble averaged values. Hence, far from the test droplet the disturbance fields, which are defined as the difference between conditionally and ensemble averaged fields, vanish. It reads,

$$\lim_{r \rightarrow \infty} \mathbf{u}_o[\mathbf{r}|\mathbf{y}, \mathbf{w}] = 0, \quad \lim_{r \rightarrow \infty} p_o[\mathbf{r}|\mathbf{y}, \mathbf{w}] = 0. \quad (2.21)$$

3 Reciprocal theorem for droplets

The reciprocal theorem for a droplet already exists in the literature; see, for example, [Lovalenti and Brady \(1993\)](#); [Raja et al. \(2010\)](#). However, [Lovalenti and Brady \(1993\)](#) focuses on the force, while [Raja et al. \(2010\)](#) focuses on the stresslet. Here, we provide a detailed derivation of the reciprocal theorem formulated to compute moments of any order for a droplet, thereby encompassing both the force and the stresslet.

3.1 Auxiliary solutions

The reciprocal theorem requires the use of a known solution. We call that solution the *auxiliary* solution, since its only purpose is to compute the *real* solution of the equations introduced above. The *auxiliary* velocity and stress fields are denoted by $\hat{\mathbf{u}}_{i/o}$ and $\hat{\boldsymbol{\sigma}}_{i/o} = -\hat{p}_{i/o} \boldsymbol{\delta} + \nabla \hat{\mathbf{u}}_{i/o} + \nabla \hat{\mathbf{u}}_{i/o}^\top$, respectively. In general, all *auxiliary* quantities are written with a hat.

In the *auxiliary* problem, we neglect all inertial effects and consider an arbitrary quadratic flow; thus $\hat{p}_{o/i}$ and $\hat{\mathbf{u}}_{o/i}$ satisfy,

$$\nabla \cdot \hat{\mathbf{u}}_o = 0, \quad \nabla \cdot \hat{\boldsymbol{\sigma}}_o = 0, \quad (3.1)$$

$$\nabla \cdot \hat{\mathbf{u}}_i = 0, \quad \nabla \cdot \hat{\boldsymbol{\sigma}}_i = 0, \quad (3.2)$$

for $r > 1$ and $r < 1$, respectively. The boundary conditions at $r \rightarrow \infty$ read,

$$\lim_{r \rightarrow \infty} \hat{\mathbf{u}}_o[\mathbf{r}|\mathbf{y}, \mathbf{w}] = 0, \quad \lim_{r \rightarrow \infty} \hat{p}_o[\mathbf{r}|\mathbf{y}, \mathbf{w}] = 0. \quad (3.3)$$

and at $r = 1$,

$$\hat{\mathbf{u}}_i = \hat{\mathbf{u}}_o \quad (3.4)$$

$$\hat{\mathbf{u}}_i \cdot \mathbf{n} = -\hat{\mathbf{w}}_r \cdot \mathbf{n} \quad (3.5)$$

$$\mathbf{n} \cdot 2[\hat{\mathbf{e}}_o - \lambda \hat{\mathbf{e}}_i + (1 - \lambda) \hat{\mathbf{E}}] \cdot (\boldsymbol{\delta} - \mathbf{n} \mathbf{n}) = \hat{\mathbf{b}} \cdot (\boldsymbol{\delta} - \mathbf{n} \mathbf{n}) \quad (3.6)$$

where we introduced $\hat{\mathbf{w}}_r = \hat{\mathbf{U}} - \mathbf{w}$ as the undisturbed relative velocity field of the *auxiliary* problem, similarly $\hat{\mathbf{E}}$ is the undisturbed shear rate of the *auxiliary* problem. Note that for the *test* problem it is important that $\hat{\mathbf{b}} \neq 0$, this will be useful to write a reciprocal relation in [Section 3](#). Indeed, this stress discontinuity is a mathematical artefact in order to evaluate the surface integral of the shear stress at the interface of the test droplet ([Raja et al., 2010](#)) but have no physical meaning here. For our purposes, we only need $\hat{\mathbf{b}}$ and $\hat{\mathbf{U}}$ to be quadratic fields. Hence, we consider the relations,

$$\hat{\mathbf{w}}_r(\mathbf{y} + \mathbf{r}) = \hat{\mathbf{U}} - \mathbf{w} + \mathbf{r} \cdot \nabla \hat{\mathbf{U}}|_{\mathbf{r}=0} + \frac{1}{2} \mathbf{r} \mathbf{r} : \nabla \nabla \hat{\mathbf{U}}|_{\mathbf{r}=0} + \dots, \quad (3.7)$$

$$\hat{\mathbf{E}}(\mathbf{y} + \mathbf{r}) = \hat{\mathbf{E}}|_{\mathbf{r}=0} + \mathbf{r} \cdot \nabla \hat{\mathbf{E}}|_{\mathbf{r}=0} + \dots, \quad (3.8)$$

$$\hat{\mathbf{b}}(\mathbf{y} + \mathbf{r}) = \hat{\mathbf{b}}|_{\mathbf{r}=0} + \mathbf{r} \cdot \nabla \hat{\mathbf{b}}|_{\mathbf{r}=0} + \frac{1}{2} \mathbf{r} \mathbf{r} : \nabla \nabla \hat{\mathbf{b}}|_{\mathbf{r}=0} + \dots. \quad (3.9)$$

According to the linearity of the Stokes equations [Eqs. \(3.1\)](#) and [\(3.2\)](#), and of the boundary conditions [Eqs. \(3.4\)](#) to [\(3.6\)](#) we deduce that $\hat{\mathbf{u}}_{i/o}$ and $\hat{p}_{i/o}$ must be linear combination of spherical harmonics proportional to $\hat{\mathbf{w}}_r|_{\mathbf{r}=0}$, $\hat{\mathbf{b}}|_{\mathbf{r}=0}$, and their derivatives ([Brenner, 1964](#)). Hence, we can write the general solution of $\mathbf{u}_{i/o}$ and $p_{i/o}$ as,

$$\begin{pmatrix} \hat{\mathbf{u}}_o \\ \hat{p}_o \\ \hat{\mathbf{u}}_i \\ \hat{p}_i \end{pmatrix} = \begin{pmatrix} \mathbb{U}_o^{(1)} + \mathbb{U}_o^{(2)} \cdot \nabla + \mathbb{U}_o^{(3)} : \nabla \nabla & \mathbb{U}_o^{(1-b)} + \mathbb{U}_o^{(2-b)} \cdot \nabla + \mathbb{U}_o^{(3-b)} : \nabla \nabla \\ \mathbb{P}_o^{(1)} + \mathbb{P}_o^{(2)} \cdot \nabla + \mathbb{P}_o^{(3)} : \nabla \nabla & \mathbb{P}_o^{(1-b)} + \mathbb{P}_o^{(2-b)} \cdot \nabla + \mathbb{P}_o^{(3-b)} : \nabla \nabla \\ \mathbb{U}_i^{(1)} + \mathbb{U}_i^{(2)} \cdot \nabla + \mathbb{U}_i^{(3)} : \nabla \nabla & \mathbb{U}_i^{(1-b)} + \mathbb{U}_i^{(2-b)} \cdot \nabla + \mathbb{U}_i^{(3-b)} : \nabla \nabla \\ \mathbb{P}_i^{(1)} + \mathbb{P}_i^{(2)} \cdot \nabla + \mathbb{P}_i^{(3)} : \nabla \nabla & \mathbb{P}_i^{(1-b)} + \mathbb{P}_i^{(2-b)} \cdot \nabla + \mathbb{P}_i^{(3-b)} : \nabla \nabla \end{pmatrix} \cdot \begin{pmatrix} \hat{\mathbf{w}}_r \\ \hat{\mathbf{b}} \end{pmatrix} \quad (3.10)$$

The tensor $\mathbb{U}_{i/o}^{(n)}$ and $\mathbb{P}_{i/o}^{(n)}$ are $n + 1$ and n order tensors given in ([Leal, 2007](#)) and in ([Fintzi and Pierson \(2025, Appendix F\)](#), that depend only on the relative coordinate $\mathbf{r} = \mathbf{x} - \mathbf{y}$ and the viscosity ratio λ . We also define the $n + 2$ order tensors,

$$\mathbb{S}_{i/o}^{(n)} = -\boldsymbol{\delta} \mathbb{P}_{i/o}^{(n)} + \nabla \mathbb{U}_{i/o}^{(n)} + {}^\dagger \nabla \mathbb{U}_{i/o}^{(n)}, \quad (3.11)$$

² where $n = 1, 2, 3$ or $1-b, 2-b, 3-b$. [Eq. \(3.11\)](#) provides the stresses fields of the *auxiliary* problem upon contraction with $\hat{\mathbf{w}}_r$, and $\hat{\mathbf{b}}$, and the higher derivatives.

3.2 Singularity solutions

Following [Stone et al. \(2001\)](#), we also consider the *auxiliary* problem of a point source located at the origin. The reason why this solution is necessary is that, in the previous *auxiliary* problem $\nabla \cdot \hat{\mathbf{U}} = 0$. Hence, as demonstrated below the previous *auxiliary*

²The † used in [Eq. \(3.11\)](#) represents the transpose operator which acts on the two closest indices. For example, the transpose of the triadic \mathbf{abc} , may be written: ${}^\dagger \mathbf{abc} = \mathbf{bac}$ or $\mathbf{abc}^\dagger = \mathbf{acb}$.

solutions are unable to provide a formula for the trace of the first moment using the reciprocal theorem. Because we also aim to compute the traces of the second moment of forces, one also need the solutions of a point force and a potential dipole. These two classes of solutions, i.e., point source and point force (and their derivatives), obey the non-homogeneous Stokes equations,

$$\nabla^2 \hat{\mathbf{u}}_o = \nabla \hat{p}_o + (\mathbf{Q}^{(n)} \odot \nabla^{(n)}) \nabla \delta(\mathbf{r}), \quad \nabla^2 \hat{\mathbf{u}}_o = \nabla \hat{p}_o + (\mathbf{R}^{(n+1)} \odot \nabla^{(n)}) \delta(\mathbf{r}), \quad (3.12)$$

respectively. Where $\mathbf{Q}^{(n)}$ and $\mathbf{R}^{(n+1)}$ are two arbitrary n^{th} and $(n+1)^{th}$ order tensors, respectively. Similarly, the $\nabla^{(n)}$ denote n^{th} order outer product of gradients vectors. The operator \odot represents the contraction product on the n^{th} common indices. Both equations are completed by the continuity equation $\nabla \cdot \mathbf{u}_o$. The solution of the point source and point force read,

$$\hat{\mathbf{u}}_o = -\frac{1}{4\pi} \nabla^{(n+1)} (1/r) \odot \mathbf{Q}^{(n)}, \quad \hat{\mathbf{u}}_o = \frac{1}{8\pi} \nabla^{(n)} [\nabla^{(2)} - \boldsymbol{\delta} \nabla^2] r \odot \mathbf{R}^{(n+1)}, \quad (3.13)$$

respectively. Note that $\frac{1}{8\pi} [\nabla^{(2)} - \boldsymbol{\delta} \nabla^2] r = -(\mathbf{n}\mathbf{n} + \boldsymbol{\delta})/(8\pi r)$ is the free-space green function of Stokes equations (Pozrikidis et al., 1992). The stress tensors read,

$$\hat{\boldsymbol{\sigma}}_o = -\frac{1}{2\pi} \nabla^{(n+2)} (1/r) \odot \mathbf{Q}^{(n)}, \quad (3.14)$$

$$\hat{\boldsymbol{\sigma}}_o = \frac{1}{8\pi} \nabla^{(n)} [2\nabla^{(3)} - (\nabla \boldsymbol{\delta} + \nabla \boldsymbol{\delta}^\dagger + \boldsymbol{\delta} \nabla) \nabla^2] r \odot \mathbf{R}^{(n+1)}, \quad (3.15)$$

for the point source and point forces solutions, respectively. More details on how to obtain those solutions are given in Pozrikidis (2011, Chapter 6) or in Section A.

As an example, the solution of a point source (i.e., Eq. (3.13) with $n = 0$) used in the calculation of the first moment of force reads,

$$\hat{\mathbf{u}}_o = \frac{Q^{(0)}}{4\pi} \mathbf{n} r^{-2}, \quad \hat{\boldsymbol{\sigma}}_o = \mu_f \frac{Q^{(0)}}{2\pi} (\boldsymbol{\delta} - 3\mathbf{n}\mathbf{n}) r^{-3} \quad (3.16)$$

Note that this expression is valid throughout the domain excluding the point $\mathbf{r} = \mathbf{x} - \mathbf{y} = 0$, hence we may use either the subscript o or i . The solution for a point source dipole ($\mathbf{Q}^{(1)}$) and point force ($\mathbf{R}^{(1)}$) will also be used to derive relations for the traces of the second moment of force. In summary, as the values of $\hat{\mathbf{w}}_r$, $\hat{\mathbf{b}}$, $\mathbf{R}^{(n)}$, and $\mathbf{Q}^{(n)}$, are entirely arbitrary, the solutions given by Eqs. (3.10), (3.13) and (3.16) can be used as a tool to derive expressions for the first and second moments of the forces by means of the reciprocal theorem derived in the next section.

3.3 Reciprocal theorem

The derivation of the general formula proceeds in three main steps: (1) we write a reciprocal relation in the exterior of the test droplet, (2) we then write the corresponding relation in the interior of the test droplet, and (3) finally, using the boundary conditions at the droplet interface, we combine the two expressions to obtain the final reciprocal relation.

3.3.1 First steps

We first take the dot product of Eq. (2.16) with $\hat{\mathbf{u}}_o$, and the dot product of Eq. (3.1) with \mathbf{u}_o , subtracting both expression gives,

$$\nabla \cdot (\boldsymbol{\sigma}_o \cdot \hat{\mathbf{u}}_o) = \nabla \cdot (\hat{\boldsymbol{\sigma}}_o \cdot \mathbf{u}_o) + Re(\hat{\mathbf{u}}_o \cdot \mathbf{f}_o). \quad (3.17)$$

To derive this relation we used the identities $\boldsymbol{\sigma}_o : \nabla \hat{\mathbf{u}}_o = 2\mathbf{e}_o : \nabla \hat{\mathbf{u}}_o = 2\mathbf{e}_o : \hat{\mathbf{e}}_o$, and $\hat{\boldsymbol{\sigma}}_o : \nabla \mathbf{u}_o = 2\hat{\mathbf{e}}_o : \mathbf{e}_o$, which imply $\boldsymbol{\sigma}_o : \nabla \hat{\mathbf{u}}_o = \hat{\boldsymbol{\sigma}}_o : \nabla \mathbf{u}_o$. This simplification explains why complete knowledge of the velocity field in the exterior of the droplet becomes unnecessary when $\mathbf{f}_o = 0$. Consequently, the power of the reciprocal theorem is rooted in the commutativity of the operation $\mathbf{e}_o : \hat{\mathbf{e}}_o$. Integrating this expression on the whole domain Ω_o , and using the divergence theorem we obtain,

$$-\oint_{\Gamma_p} \hat{\mathbf{u}}_o \cdot \boldsymbol{\sigma}_o \cdot \mathbf{n} d\Gamma = -\oint_{\Gamma_p} \mathbf{u}_o \cdot \hat{\boldsymbol{\sigma}}_o \cdot \mathbf{n} d\Gamma + Re \int_{\Omega_o} \hat{\mathbf{u}}_o \cdot \mathbf{f}_o d\Omega. \quad (3.18)$$

The surface integrals appears only on the boundary of the test droplet because far from the test droplet ($r \rightarrow \infty$), the fields $\hat{\mathbf{u}}_o$, $\hat{\boldsymbol{\sigma}}_o$, \mathbf{u}_o and $\boldsymbol{\sigma}_o$ vanish (see Eq. (2.21) and Eq. (3.3)). Eq. (3.18) already provides a sufficient reciprocal relation when considering solid particles (Masoud and Stone, 2019). Indeed, in that case $\mathbf{u}_o = -\mathbf{w}_r$, and $\hat{\mathbf{u}}_o = -\hat{\mathbf{w}}_r$ at $r = 1$, because of the no-slip boundary condition at the particle interface, hence leading directly to a formula for the force traction on the surface of the solid particle (first term on the left-hand side of Eq. (3.19)). Of course, one still needs to provide an approximation for \mathbf{f}_o if inertia is considered. For fluid particles, a few more steps are necessary. Inserting the relation $\mathbf{u}_o = \mathbf{u}_o + \mathbf{w}_r - \mathbf{w}_r$ and $\hat{\mathbf{u}}_o = \hat{\mathbf{u}}_o + \hat{\mathbf{w}}_r - \hat{\mathbf{w}}_r$ gives,

$$\begin{aligned} & \oint_{\Gamma_p} \hat{\mathbf{w}}_r \cdot \boldsymbol{\sigma}_o \cdot \mathbf{n} d\Gamma - 2 \oint_{\Gamma_p} (\hat{\mathbf{u}}_o + \hat{\mathbf{w}}_r) \cdot \mathbf{e}_o \cdot \mathbf{n} d\Gamma \\ &= \oint_{\Gamma_p} \mathbf{w}_r \cdot \hat{\boldsymbol{\sigma}}_o \cdot \mathbf{n} d\Gamma - 2 \oint_{\Gamma_p} (\mathbf{u}_o + \mathbf{w}_r) \cdot \hat{\mathbf{e}}_o \cdot \mathbf{n} d\Gamma + Re \int_{\Omega_o} \hat{\mathbf{u}}_o \cdot \mathbf{f}_o d\Omega. \end{aligned} \quad (3.19)$$

Where we used the relation, $(\hat{\mathbf{u}}_o + \hat{\mathbf{w}}_r) \cdot \boldsymbol{\sigma}_o \cdot \mathbf{n} = 2(\hat{\mathbf{u}}_o + \hat{\mathbf{w}}_r) \cdot \mathbf{e}_o \cdot \mathbf{n}$, allowed because $(\hat{\mathbf{u}}_o + \hat{\mathbf{w}}_r) = (\boldsymbol{\delta} - \mathbf{n}\mathbf{n}) \cdot (\hat{\mathbf{u}}_o + \hat{\mathbf{w}}_r)$ on the surface of the test droplet, see Eq. (3.5). Similar considerations lead to $(\mathbf{u}_o + \mathbf{w}_r) \cdot \hat{\boldsymbol{\sigma}}_o \cdot \mathbf{n} = 2(\mathbf{u}_o + \mathbf{w}_r) \cdot \hat{\mathbf{e}}_o \cdot \mathbf{n}$.

3.3.2 Intermediate steps

The equations governing the flow inside the droplets have not yet been considered. We now take the dot product of Eq. (2.18) with $(\hat{\mathbf{u}}_i + \hat{\mathbf{w}}_r)$ and of Eq. (3.2) with $(\mathbf{u}_i + \mathbf{w}_r)$, subtracting both expression leads to,

$$\nabla \cdot [\boldsymbol{\sigma}_i \cdot (\hat{\mathbf{u}}_i + \hat{\mathbf{w}}_r)] - 2\mathbf{e}_i : \hat{\mathbf{E}} = \nabla \cdot [\hat{\boldsymbol{\sigma}}_i \cdot (\mathbf{u}_i + \mathbf{w}_r)] - 2\hat{\mathbf{e}}_i : \mathbf{E} + (\hat{\mathbf{u}}_i + \hat{\mathbf{w}}_r) \cdot \mathbf{f}_i^{tot}, \quad (3.20)$$

where we used the relation, $-\boldsymbol{\sigma}_i : \nabla(\hat{\mathbf{u}}_i + \hat{\mathbf{w}}_r) + \hat{\boldsymbol{\sigma}}_i : \nabla(\mathbf{u}_i + \mathbf{w}_r) = -2\mathbf{e}_i : \hat{\mathbf{E}} + 2\hat{\mathbf{e}}_i : \mathbf{E}$. Integrating this relation over the domain Ω_i , and using the divergence theorem, as well

as similar simplifications used in Eq. (3.19), gives,

$$\begin{aligned} & \oint_{\Gamma_p} (\hat{\mathbf{u}}_i + \hat{\mathbf{w}}_r) \cdot \mathbf{e}_i \cdot \mathbf{n} d\Gamma - \int_{\Omega_i} \mathbf{e}_i : \hat{\mathbf{E}} d\Omega \\ &= \oint_{\Gamma_p} (\mathbf{u}_i + \mathbf{w}_r) \cdot \hat{\mathbf{e}}_i \cdot \mathbf{n} d\Gamma - \int_{\Omega_i} \hat{\mathbf{e}}_i : \hat{\mathbf{E}} d\Omega + \frac{1}{2} \int_{\Omega_i} (\hat{\mathbf{u}}_i + \hat{\mathbf{w}}_r) \cdot \mathbf{f}_i^{tot} d\Omega \end{aligned} \quad (3.21)$$

The first terms on both the left- and right-hand sides of Eq. (3.21) may be obtained using Eq. (2.20) and Eq. (3.21). Indeed, since $(\hat{\mathbf{u}}_i + \hat{\mathbf{w}}_r) \cdot (\boldsymbol{\delta} - \mathbf{n}\mathbf{n}) = (\hat{\mathbf{u}}_i + \hat{\mathbf{w}}_r)$, multiplying Eq. (2.20) by $(\hat{\mathbf{u}}_i + \hat{\mathbf{w}}_r)$ yields

$$-2\lambda(\hat{\mathbf{u}}_{i/o} + \hat{\mathbf{w}}_r) \cdot \mathbf{e}_i \cdot \mathbf{n} = \mathbf{b} \cdot (\hat{\mathbf{u}}_{i/o} + \hat{\mathbf{w}}_r) - 2(\hat{\mathbf{u}}_{i/o} + \hat{\mathbf{w}}_r) \cdot \mathbf{e}_o \cdot \mathbf{n} - 2(1-\lambda)(\hat{\mathbf{u}}_{i/o} + \hat{\mathbf{w}}_r) \cdot \mathbf{E} \cdot \mathbf{n} \quad (3.22)$$

with a similar relation for the *test* problem boundary condition. Adding Eq. (3.19) and Eq. (3.21) times 2λ , while using the boundary condition given by Eq. (3.22) leads to the expression,

$$\begin{aligned} & \oint_{\Gamma_p} \hat{\mathbf{w}}_r \cdot \boldsymbol{\sigma}_o \cdot \mathbf{n} d\Gamma - \lambda \int_{\Omega_i} 2\mathbf{e}_i : \hat{\mathbf{E}} d\Omega - (1-\lambda) \oint_{\Gamma_p} 2(\mathbf{u}_i + \mathbf{w}_r) \cdot \hat{\mathbf{E}} \cdot \mathbf{n} d\Gamma + \oint_{\Gamma_p} (\mathbf{u}_i + \mathbf{w}_r) \cdot \hat{\mathbf{b}} d\Gamma \\ &= \oint_{\Gamma_p} \mathbf{w}_r \cdot \hat{\boldsymbol{\sigma}}_o \cdot \mathbf{n} d\Gamma - \lambda \int_{\Omega_i} 2\hat{\mathbf{e}}_i : \hat{\mathbf{E}} d\Omega - (1-\lambda) \oint_{\Gamma_p} 2(\hat{\mathbf{u}}_i + \hat{\mathbf{w}}_r) \cdot \mathbf{E} \cdot \mathbf{n} d\Gamma \\ &+ \oint_{\Gamma_p} (\hat{\mathbf{u}}_i + \hat{\mathbf{w}}_r) \cdot \mathbf{b} d\Gamma + \lambda \int_{\Omega_i} (\hat{\mathbf{u}}_i + \hat{\mathbf{w}}_r) \cdot \mathbf{f}_i^{tot} d\Omega + Re \int_{\Omega_o} \hat{\mathbf{u}}_o \cdot \mathbf{f}_o d\Omega. \end{aligned} \quad (3.23)$$

3.4 Final steps

To obtain the final form of the reciprocal theorem, we proceed by noting that the second and third terms on the left-hand side of Eq. (3.23) may be combined upon using the divergence theorem on the third term, and using the relation,

$$-\lambda \mathbf{e}_i : \hat{\mathbf{E}} - (1-\lambda) \nabla \cdot [\hat{\mathbf{E}} \cdot (\mathbf{u}_i + \mathbf{w}_r)] = -\mathbf{e}_i : \hat{\mathbf{E}} - (1-\lambda) \hat{\mathbf{E}} : \mathbf{E} - (1-\lambda) \nabla \cdot \hat{\mathbf{E}} \cdot (\mathbf{u}_i + \mathbf{w}_r). \quad (3.24)$$

One can also derive the same manipulation on the second and third term on the right-hand side of Eq. (3.23), namely,

$$-\lambda \hat{\mathbf{e}}_i : \mathbf{E} - (1-\lambda) \nabla \cdot [\mathbf{E} \cdot (\hat{\mathbf{u}}_i + \hat{\mathbf{w}}_r)] = -\hat{\mathbf{e}}_i : \mathbf{E} - (1-\lambda) \hat{\mathbf{E}} : \mathbf{E} - (1-\lambda) \nabla \cdot \mathbf{E} \cdot (\hat{\mathbf{u}}_i + \hat{\mathbf{w}}_r). \quad (3.25)$$

Because the product $\hat{\mathbf{E}} : \mathbf{E}$ is commutative, the second term on the right-hand side of Eqs. (3.24) and (3.25) cancel each other in the final expression. Injecting both Eqs. (3.24) and (3.25) in Eq. (3.23) leads to the final form of the reciprocal theorem for droplets, namely

$$\begin{aligned} & \oint_{\Gamma_p} \hat{\mathbf{w}}_r \cdot \boldsymbol{\sigma}_o \cdot \mathbf{n} d\Gamma - \int_{\Omega_i} 2\mathbf{e}_i : \nabla \hat{\mathbf{U}} d\Omega - (1-\lambda) \int_{\Omega_i} (\mathbf{u}_i + \mathbf{w}_r) \cdot \nabla^2 \hat{\mathbf{U}} d\Omega + \oint_{\Gamma_p} (\mathbf{u}_i + \mathbf{w}_r) \cdot \hat{\mathbf{b}} d\Gamma \\ &= \oint_{\Gamma_p} \mathbf{w}_r \cdot \hat{\boldsymbol{\sigma}}_o \cdot \mathbf{n} d\Gamma - \int_{\Omega_i} 2\hat{\mathbf{e}}_i : \nabla \mathbf{U} d\Omega - (1-\lambda) \int_{\Omega_i} (\hat{\mathbf{u}}_i + \hat{\mathbf{w}}_r) \cdot \nabla^2 \mathbf{U} d\Omega \\ &+ \oint_{\Gamma_p} (\hat{\mathbf{u}}_i + \hat{\mathbf{w}}_r) \cdot \mathbf{b} d\Gamma + \lambda \int_{\Omega_i} (\hat{\mathbf{u}}_i + \hat{\mathbf{w}}_r) \cdot \mathbf{f}_i^{tot} d\Omega + Re \int_{\Omega_o} \hat{\mathbf{u}}_o \cdot \mathbf{f}_o d\Omega. \end{aligned} \quad (3.26)$$

Table 1: Configurations of the *auxiliary* problem. Configuration 1 is used to compute the force; Configurations 2 and 3 to compute the first moment of the force; Configurations 4-6 to compute the second moment of the force; and Configuration 4 to compute the droplet internal shear rate.

Configurations	$\hat{\mathbf{w}}_r(\mathbf{x})$	$\hat{\mathbf{b}}(\mathbf{x})$	Point source / force solutions
1	$\hat{\mathbf{w}}_r[\mathbf{r}] = \hat{\mathbf{w}}_r$	$\hat{\mathbf{b}}[\mathbf{r}] = 0$	$\mathbf{Q}^{(n)} = 0, \mathbf{R}^{(n)} = 0$
2	$\hat{\mathbf{w}}_r[\mathbf{r}] = \mathbf{r} \cdot \nabla \hat{\mathbf{U}}$	$\hat{\mathbf{b}}[\mathbf{r}] = 0$	$\mathbf{Q}^{(n)} = 0, \mathbf{R}^{(n)} = 0$
3	$\hat{\mathbf{w}}_r[\mathbf{r}] = \mathbf{0}$	$\hat{\mathbf{b}}[\mathbf{r}] = 0$	$Q^{(0)}$
4	$\hat{\mathbf{w}}_r[\mathbf{r}] = \frac{1}{2}\mathbf{r}\mathbf{r} \cdot \nabla \nabla \hat{\mathbf{U}}$	$\hat{\mathbf{b}}[\mathbf{r}] = 0$	$\mathbf{Q}^{(n)} = 0, \mathbf{R}^{(n)} = 0$
5	$\hat{\mathbf{w}}_r[\mathbf{r}] = \mathbf{0}$	$\hat{\mathbf{b}}[\mathbf{r}] = 0$	$\mathbf{Q}^{(1)}$
6	$\hat{\mathbf{w}}_r[\mathbf{r}] = \mathbf{0}$	$\hat{\mathbf{b}}[\mathbf{r}] = 0$	$\mathbf{R}^{(1)}$
7	$\hat{\mathbf{w}}_r[\mathbf{r}] = 0$	$\hat{\mathbf{b}}[\mathbf{r}] = \hat{\mathbf{b}}$	$\mathbf{Q}^{(n)} = 0, \mathbf{R}^{(n)} = 0$

Note that we used the relations, $2\mathbf{e}_i : \hat{\mathbf{E}} = 2\mathbf{e}_i : \nabla \hat{\mathbf{U}}$ and $\nabla \cdot \mathbf{E} = \frac{1}{2}\nabla^2 \mathbf{U}$ because the background flow is divergence free (Eq. (2.2)). Upon making the good choice for $\hat{\mathbf{w}}_r$ and $\hat{\mathbf{b}}$ (i.e. whether it is constant, linear, or quadratic, see Eq. (3.7)), one recovers on the left-hand side of Eq. (3.26) the expression of the force, first, and second moments applied on the droplet in a yet arbitrary flow described by \mathbf{w}_r and \mathbf{b} , and their gradients.

On the right-hand side of Eq. (3.26) all the terms are either known quantities from the *auxiliary* problem ($\hat{\boldsymbol{\sigma}}_o, \hat{\mathbf{e}}_i, \hat{\mathbf{u}}_{i/o/r}$), or boundary conditions of the “real” problem (\mathbf{U}, \mathbf{w}_r and \mathbf{b}). However, one exception remains, that is the inertial term \mathbf{f}_o (resp. \mathbf{f}_i^{tot}), which is a function of the unknown velocity field \mathbf{u}_o (resp. \mathbf{u}_i). Hence, to compute the right-hand side of Eq. (3.26), we must use some approximations allowing us to compute the last two terms of Eq. (3.26) without the knowledge of the complete solution. This is the subject of the next section.

4 Moments of forces on a translating droplet

In this section, we provide the general formulation for the drag force, first moments of forces, and second moments of forces, as appearing in Eqs. (2.8) and (2.10). Once these formulas are properly established, we will consider the case of a droplet embedded in a steady uniform flow (i.e., when $\mathbf{w}_r[\mathbf{r}, t] = \mathbf{w}_r$ is a steady and uniform vector field) at a small but finite Reynolds number.

4.1 Formulas for the force, first, and second moments

Let us consider the configurations of the *auxiliary* problem listed Table 1. For any of configurations: 1 through 7, the expressions for $\hat{\boldsymbol{\sigma}}_{i/o}$ and $\hat{\mathbf{u}}_{i/o}$ required in Eq. (3.26) can be obtained from Eqs. (3.10), (3.11) and (3.16).

Substituting configuration 1 into Eq. (3.26) and factoring out $\hat{\mathbf{w}}_r$ yields,

$$\oint_{\Gamma_p} \boldsymbol{\sigma}_o \cdot \mathbf{n} d\Gamma = \oint_{\Gamma_p} \mathbf{w}_r \cdot \mathbb{S}_o^{(1)} \cdot \mathbf{n} d\Gamma - \int_{\Omega_i} \mathbb{S}_i^{(1)} : \nabla \mathbf{U} d\Omega - (1 - \lambda) \int_{\Omega_i} (\mathbb{U}_i^{(1)} + \boldsymbol{\delta}) \cdot \nabla^2 \mathbf{U} d\Omega \\ + \oint_{\Gamma_p} (\mathbb{U}_{i/o}^{(1)} + \boldsymbol{\delta}) \cdot \mathbf{b} d\Gamma + \lambda \int_{\Omega_i} (\mathbb{U}_i^{(1)} + \boldsymbol{\delta}) \cdot \mathbf{f}_i^{tot} d\Omega + Re \int_{\Omega_o} \mathbb{U}_o^{(1)} \cdot \mathbf{f}_o d\Omega, \quad (4.1)$$

which is a general formula for the hydrodynamic drag forces. Based on this formula, one can re-derive Faxen law, for example (Stone et al., 2001).

The general formula for the first moment of force may be obtained by setting configuration 2 into Eq. (3.26), it yields,

$$\oint_{\Gamma_p} r_j (\boldsymbol{\sigma}_o \cdot \mathbf{n})_i d\Gamma - \int_{\Omega_i} 2(\mathbf{e}_i)_{ij} d\Omega \stackrel{i \neq j}{=} \oint_{\Gamma_p} (\mathbf{w}_r)_l (\mathbb{S}_o^{(2)})_{ijkl} n_k d\Gamma - \int_{\Omega_i} (\mathbb{S}_i^{(2)})_{ijkl} (\nabla \mathbf{U})_{kl} d\Omega \\ + (\zeta - 1) \int_{\Omega_i} (\mathbb{U}_i^{(2)} + \mathbf{r}\boldsymbol{\delta})_{ijk} (\nabla^2 \mathbf{U})_k d\Omega + \oint_{\Gamma_p} (\mathbb{U}_i^{(2)} + \mathbf{r}\boldsymbol{\delta})_{ijk} b_k d\Gamma \\ + \lambda \int_{\Omega_i} (\mathbb{U}_i^{(2)} + \mathbf{r}\boldsymbol{\delta})_{ijk} (\mathbf{f}_i^{tot})_k d\Omega + Re \int_{\Omega_o} (\mathbb{U}_o^{(2)})_{ijk} (\mathbf{f}_o)_k d\Omega, \quad (4.2)$$

It is important to note that to derive Eq. (4.2) we have factorized the equations by the tensor $(\nabla \hat{\mathbf{U}})_{ij}$. Because $(\nabla \hat{\mathbf{U}})_{kk} = \nabla \cdot \hat{\mathbf{U}} = 0$, taking the trace of Eq. (4.2) leads to an incorrect expression, since it would mean factoring by zero. Therefore, it is important to note that this equality holds only for $i \neq j$. Hence, if we note \mathbb{M}_{ij} the whole first moment, then Eq. (4.2) only provides its traceless part, namely: $\mathbb{M}_{ij} - 1/3\delta_{ij}\mathbb{M}_{kk}$. Nevertheless, using configuration 3 in Eq. (3.18), we obtain a formula for the trace of the first moment (\mathbb{M}_{kk}), which reads,

$$\oint_{\Gamma_p} \mathbf{r} \cdot \boldsymbol{\sigma}_o \cdot \mathbf{n} d\Gamma = -Re \int_{\Omega_o} \frac{\mathbf{r}}{r^3} \cdot \mathbf{f}_o d\Omega. \quad (4.3)$$

Indeed, the integral of $\mathbf{u}_o \cdot \hat{\boldsymbol{\sigma}}_o$ over the droplet surface on the right-hand side of Eq. (3.17) vanishes because $\mathbf{u}_o \cdot \hat{\boldsymbol{\sigma}}_o \propto \mathbf{u}_o \cdot \mathbf{n}$ at $r = 1$, and \mathbf{u}_o is divergence-free (Stone et al., 2001). By adding δ_{ij} times Eq. (4.3) to the traceless part of Eq. (4.3), one obtains an expression valid for every pair of indices i and j , that is, the complete first-moment tensor.

Using configuration 4 (see Table 1), we obtain the general relation for the second moment of the force (in index notation),

$$\frac{1}{2} \oint_{\Gamma_p} (\boldsymbol{\sigma}_o \cdot \mathbf{n})_i r_j r_k d\Gamma - \int_{\Omega_i} 2(\mathbf{e}_i)_{ij} r_k d\Omega \stackrel{i \neq j, k}{=} \oint_{\Gamma_p} (\mathbf{w}_r)_l (\mathbb{S}_o^{(3)})_{ijklm} n_m d\Gamma - \int_{\Omega_i} (\mathbb{S}_o^{(3)})_{ijklm} (\nabla \mathbf{U})_{lm} d\Omega \\ - (1 - \lambda) \int_{\Omega_i} ((\mathbf{U}_i^{(3)})_{ijkl} + \frac{1}{2} r_k r_l \delta_{il}) (\nabla^2 \mathbf{U})_l d\Omega + \oint_{\Gamma_p} ((\mathbf{U}_i^{(3)})_{ijkl} + \frac{1}{2} r_k r_l \delta_{il}) b_l d\Gamma \\ + \lambda \int_{\Omega_i} ((\mathbf{U}_i^{(3)})_{ijkl} + \frac{1}{2} r_k r_l \delta_{il}) (\mathbf{f}_i^{tot})_l d\Omega + Re \int_{\Omega_o} (\mathbf{U}_i^{(3)})_{ijkl} \cdot \mathbf{f}_o d\Omega, \quad (4.4)$$

Where we used the relation: $\int_{\Omega_i} (\mathbf{u}_i + \mathbf{w}_r) d\Omega = \mathbf{w} - \mathbf{w} = 0$. This formula is valid for a droplet immersed in an otherwise arbitrary background flow with velocity \mathbf{U} and an interfacial jump \mathbf{b} . However, it is only valid for $i \neq j, k$. Indeed, we have factored out

$(\nabla \nabla \hat{\mathbf{U}})_{kji}$, and $(\nabla \nabla \hat{\mathbf{U}})_{kii} = (\nabla \nabla \hat{\mathbf{U}})_{iji} = 0$. Consequently, if we denote by \mathbb{K}_{ijk} the complete second moment, Eq. (4.22) provides only the traceless part of \mathbb{K}_{ijk} under any contraction over i, j or i, k . Therefore, a separate expression is still required for the trace of Eq. (4.4), together with a procedure to combine this trace with the previously undefined traceless part (with respect to i, j and i, k) of \mathbb{K}_{ijk} . This procedure is detailed in Section B.1 and yields to

$$\mathbb{G}_{ijk} = \mathbb{K}_{ijk} + \frac{1}{8}(\mathbb{K}_{lkl}\delta_{ij} - 3\mathbb{K}_{llk})\delta_{ij} + \frac{1}{8}(\mathbb{K}_{llj} - 3\mathbb{K}_{ljl})\delta_{ik} \quad (4.5)$$

One can verify that taking the trace of this expression over (i, k) or (i, j) yields zero. To obtain the whole second moment from G_{ijk} (i.e. from Eq. (4.4)) we use the relation,

$$\mathbb{K}_{ijk} = \mathbb{G}_{ijk} + \frac{1}{8}(3\mathbb{K}_{llk} - \mathbb{K}_{lkl})\delta_{ij} + \frac{1}{8}(3\mathbb{K}_{ljl} - \mathbb{K}_{llj})\delta_{ik}, \quad (4.6)$$

where \mathbb{G} is defined as the traceless part of \mathbb{K} under contractions over the index pairs ij and ik . To obtain the traces of the second moment, i.e., \mathbb{K}_{lkl} and \mathbb{K}_{llk} , we can use a procedure similar to the one used for Eq. (4.3). For the moment, we delay this procedure to the next section, where the real problem will be defined in greater detail.

Recall that $\boldsymbol{\sigma}_o$ and \mathbf{e}_i are the local stress and shear rate, relative to the bulk stress ($\boldsymbol{\Sigma}$), and bulk shear rate (\mathbf{E}), respectively. Consequently, the left-hand side of Eqs. (4.1) to (4.4) are exactly the terms we seek in Eqs. (2.8) and (2.10).

Although these formulas are sufficient to close the averaged momentum equations, one may be interested into the expression for the integral of \mathbf{e}_i over the droplet volume, independently of the integral of $\mathbf{r}\boldsymbol{\sigma}_o \cdot \mathbf{n}$, in opposition to Eq. (4.2) which provide the sum of these two terms. Indeed, this term can be used for the calculation of the droplet deformation, see for example Fintzi and Pierson (2025). Using the configuration 7 of Table 1 we obtain:

$$\oint_{\Gamma_p} (\mathbf{u}_i + \mathbf{w}_r) \mathbf{r} d\Gamma = \oint_{\Gamma_p} \mathbf{w}_r \cdot \mathbb{S}_o^{(2-b)} \cdot \mathbf{n} d\Gamma - \int_{\Omega_i} \mathbb{S}_o^{(2-b)} : \nabla \mathbf{U} d\Omega + (\zeta - 1) \int_{\Omega_i} \mathbb{U}_i^{(2-b)} \cdot \nabla^2 \mathbf{U} d\Omega \\ + \oint_{\Gamma_p} \mathbb{U}_i^{(2-b)} \cdot \mathbf{b} d\Gamma + \lambda \int_{\Omega_i} \mathbb{U}_i^{(2-b)} \cdot \mathbf{f}_i^{tot} d\Omega + Re \int_{\Omega_o} \mathbb{U}_o^{(2-b)} \cdot \mathbf{f}_o d\Omega. \quad (4.7)$$

Upon using the divergence theorem on the left-hand side term, one can obtain a formula for the integral of the droplet internal gradient of velocity, which symmetric part corresponds to twice the integral of \mathbf{e}_i over the droplet volume.

4.2 Force moments on a droplet immersed in a steady uniform flow at low Reynolds number

This subsection considers only a uniform steady state relative motion in the *real* problem, such that $\mathbf{w}_r = \mathbf{U} - \mathbf{w}$ is not a function of space and time. Furthermore we assume clean interfaces, such that $\mathbf{b} = \mathbf{0}$.

4.2.1 Oseen drag force

In this section, we show how to obtain the $O(Re)$ correction to the drag force on a translating spherical droplet using the reciprocal theorem. Although this result has

been known for a long time (Taylor and Acrivos, 1964), the present derivation allows us to introduce useful notation and to clarify the methodology employed in the subsequent sections. Using Eq. (4.1), we obtain

$$\oint_{\Gamma_p} \boldsymbol{\sigma}_o \cdot \mathbf{n} d\Gamma = \mathbf{w}_r \cdot \oint_{\Gamma_p} \mathbb{S}_o^{(1)} \cdot \mathbf{n} d\Gamma + \zeta Re \int_{\Omega_i} (\mathbb{U}_i^{(1)} + \boldsymbol{\delta}) \cdot \mathbf{f}_i d\Omega + Re \int_{\Omega_o} \mathbb{U}_o^{(1)} \cdot \mathbf{f}_o d\Omega. \quad (4.8)$$

The term involving the divergence of mean stress, cancelled out because the latter is a constant vector in this configuration and $\int_{\Omega_i} \mathbf{w}_r + \mathbf{u}_i d\Omega = 0$. The first term on the right-hand side is by definition the Stokes flow contribution to the drag, since $\mathbf{w}_r \cdot \mathbb{S}_o^{(1)}$ represents the stress field of a translating spherical droplet in Stokes flow condition (Eq. (3.10)). Thus,

$$\mathbf{w}_r \cdot \oint_{\Gamma_p} \mathbb{S}_o^{(1)} \cdot \mathbf{n} d\Gamma = 2\pi \frac{2+3\lambda}{\lambda+1} \mathbf{w}_r = \mathbf{f}, \quad (4.9)$$

where we introduced the vector \mathbf{f} as a shorthand for the dimensionless Stokes drag force.

The real challenge is to compute the last two integrals on the right-hand side of Eq. (4.8), which require an expression for the forcing term \mathbf{f}_o and \mathbf{f}_i . In a situation where only steady and uniform relative motions are present, we deduce from Eqs. (2.16) and (2.18) that,

$$\mathbf{f}_{i/o} = (\mathbf{u}_{i/o} + \mathbf{w}_r) \cdot \nabla \mathbf{u}_{i/o}, \quad (4.10)$$

where we recall that $\mathbf{u}_{i/o}$ is the yet unknown velocity fields inside or outside the translating droplet. To obtain the $O(Re)$ correction to the drag force, one only needs to obtain a uniformly valid approximation of $\mathbf{f}_{i/o}$ accurate at $O(1)$ in Re . It is well known that the fields $\mathbf{u}_{i/o}$, can be approximated by $\mathbf{u}_{i/o} \approx \mathbb{U}_{i/o}^{(1)} \cdot \mathbf{w}_r$ only at distance $r < O(Re^{-1})$ (Kaplin and Lagerstrom, 1957; Proudman and Pearson, 1957). Otherwise, for $r > O(Re^{-1})$, one may use the velocity field generated by a point force in the Oseen equation, i.e., the solution of (Pozrikidis, 2011),

$$-\nabla p_{out} + \nabla^2 \mathbf{u}_{out} + \mathbf{f}\delta(\mathbf{r}) = Re \mathbf{w}_r \cdot \nabla \mathbf{u}_{out}, \quad (4.11)$$

where p_{out} and \mathbf{u}_{out} are the out pressure and velocity fields. This equation may be solved in the sense of generalized functions (Pozrikidis, 2011, Chapter 6), or with the use of Fourier transform (Candelier and Mehlitz, 2016), it gives $\mathbf{u}_{out} = \mathbb{U}^{(out)} \cdot \mathbf{f}$, with,

$$\mathbb{U}^{(out)} = \frac{e^X}{4\pi r} \boldsymbol{\delta} + \nabla \left(\frac{e^X - 1}{8\pi} (\mathbf{w}_r - \mathbf{n}) \right), \quad (4.12)$$

where $X = \frac{Re}{2} r (\mathbf{w}_r \cdot \mathbf{n} - 1)$. Recall that \mathbf{w}_r is the dimensionless relative velocity vector, hence it is a unit vector.

The last term on the right-hand side of Eq. (4.1) can now be evaluated as,

$$\begin{aligned} \int_{\Omega_o} \mathbb{U}_o^{(1)} \cdot \mathbf{f}_o d\Omega &= \int_{1 < |\mathbf{r}| < Re^{-1}} \mathbb{U}_o^{(1)} \cdot (\mathbb{U}_o^{(1)} + \boldsymbol{\delta}) \cdot \nabla \mathbb{U}_o^{(1)} d^3 \mathbf{r} : \mathbf{w}_r \mathbf{w}_r, \\ &+ \int_{1 < |\mathbf{r}| < \infty} \mathbb{U}_o^{(1)} \cdot (\mathbf{u}_{out} + \mathbf{w}_r) \cdot \nabla \mathbf{u}_{out} d^3 \mathbf{r}, \end{aligned} \quad (4.13)$$

where we have used the inner solution in the region $r < Re^{-1}$ and the outer solution otherwise. The outer solution is integrated from 1 rather than from Re^{-1} because it also accounts for the $O(Re)$ correction from the first-order inner velocity field. This is justified since the inner solution at $O(Re)$ matches the Oseen solution at large r , so the Oseen solution effectively ‘contains’ part of the first-order inner solution (Masoud and Stone, 2019). Because $\mathbb{U}_o^{(1)}$ is an even function of \mathbf{n} and $\nabla \mathbb{U}_o^{(1)}$ an odd function of \mathbf{n} , the product, $\mathbb{U}_o^{(1)} \cdot (\mathbb{U}_o^{(1)} + \boldsymbol{\delta}) \cdot \nabla \mathbb{U}_o^{(1)}$ is odd in \mathbf{n} . Thus, this term vanishes upon integration over the spherical surface centred at the origin. Hence, the inner solution does not contribute to the $O(Re)$ correction to the drag force. The integral of $(\mathbb{U}_i^{(1)} + \boldsymbol{\delta}) \cdot \mathbf{f}_i$ over Ω_i , in Eq. (4.1), vanishes for similar reasons.

The second integral of Eq. (4.13) represents the contribution of the outer solution. Before integration, it is useful to make the change of variables: $\tilde{\mathbf{r}} = R\mathbf{r}$. Doing so for every term in the second integral of Eq. (4.13) yields numerous simplifications because it makes appear the Reynolds number explicitly in the expression. In particular, the term $\mathbf{u}_{out} \cdot \nabla \mathbf{u}_{out}$ is of order $o(Re)$ and is therefore negligible. Moreover, $\mathbb{U}_o^{(1)} Re^{-1} = |\mathbf{f}| \cdot \tilde{\mathbb{G}}(\tilde{\mathbf{r}}) + O(Re)$ where $\tilde{\mathbb{G}} = (\boldsymbol{\delta} + \mathbf{n}\mathbf{n})(8\pi\tilde{r})^{-1}$ is the Green function of Stokes flows, written in stretched coordinates. The Green function written in standard coordinates will also be denoted by $\mathbb{G} = (\boldsymbol{\delta} + \mathbf{n}\mathbf{n})(8\pi r)^{-1}$. Then one can show that,

$$\begin{aligned} \int_{1 < |\mathbf{r}| < \infty} \mathbb{U}_o^{(1)} \cdot (\mathbf{u}_{out} + \mathbf{w}_r) \cdot \nabla \mathbf{u}_{out} d^3\mathbf{r} &= \mathbf{f} \cdot \mathbf{f} : \int_{Re < |\tilde{\mathbf{r}}| < \infty} \nabla \tilde{\mathbb{U}}_o^{(out)} \cdot \tilde{\mathbb{G}} d^3\tilde{\mathbf{r}} \\ &= \mathbf{w}_r \frac{(\mathbf{f} \cdot \mathbf{f})}{16\pi} + O(Re). \end{aligned} \quad (4.14)$$

The integral written in stretched coordinates (Eq. (4.14)) is usually evaluated using the Fourier convolution theorem (see Stone et al. (2001)). Here, we carried out the direct integration in spherical coordinates. We have used the open-source library `sympy` of Python to compute this integral and the subsequent ones in this work. Finally, by using Eqs. (4.9) and (4.14) in Eq. (4.8) we obtain the drag force on the droplet as,

$$\oint_{\Gamma_p} \boldsymbol{\sigma}_o \cdot \mathbf{n} d\Gamma = \mathbf{f} + \frac{Re}{16\pi} (\mathbf{f} \cdot \mathbf{f}) \mathbf{w}_r = 2\pi \frac{2+3\lambda}{\lambda+1} \mathbf{w}_r + \pi \frac{(2+3\lambda)^2}{(\lambda+1)^2} \frac{Re}{4} \mathbf{w}_r. \quad (4.15)$$

We recovered the classic results derived by Taylor and Acrivos (1964).

4.2.2 First moment of force

The first moment may be computed directly from Eqs. (4.1) and (4.3). The former equation reads,

$$\oint_{\Gamma_p} r_j (\boldsymbol{\sigma}_o \cdot \mathbf{n})_i d\Gamma - \int_{\Omega_i} 2(\mathbf{e}_i)_{ij} d\Omega \stackrel{i \neq j}{=} \zeta Re \int_{\Omega_i} (\mathbb{U}_i^{(2)} + \mathbf{r}\boldsymbol{\delta})_{ijk} (\mathbf{f}_i)_k d\Omega + Re \int_{\Omega_o} (\mathbb{U}_o^{(2)})_{ijk} (\mathbf{f}_o)_k d\Omega, \quad (4.16)$$

where we noticed that $\oint_{\Gamma_p} \mathbb{S}^{(2)} \cdot \mathbf{n} d\Gamma = 0$, whence the right-hand side of Eqs. (4.3) and (4.16) only contains inertial contributions. This is because the Stresslet on a translating droplet in pure Stokes flow is zero (Kim and Karrila, 2013).

We now focus on computing the last inertial term on the right-hand side of Eq. (4.16), which involves the forcing term \mathbf{f}_o , still given by Eq. (4.10). It is found that the outer

contribution to this integral is negligible at leading order in Re , and in this case the $O(Re)$ inertial effects can be obtained through a regular perturbation procedure. Indeed, in the far field, the forcing term \mathbf{f}_o scales as $1/r$, while $\mathbb{U}_o^{(2)} \sim r^{-3}$. Consequently, the integrand associated with the stresslet scales as $O(1/r^4)$, implying convergence of the integral at large r . The convergence of the volume integrals indicates the regular nature of the inertial contribution (Dabade et al., 2015). This can also be understood by introducing stretched coordinates ($\mathbf{r} \rightarrow Re^{-1}\tilde{\mathbf{r}}$), in which case $\mathbb{U}^{(2)} \sim Re^3\tilde{r}^{-3}$. If $\mathbb{U}_o^{(1)}$ is replaced by $\mathbb{U}^{(2)}$ in Eq. (4.14), it becomes clear that the resulting integrand cannot be of $O(1)$. Similar arguments are presented in Stone et al. (2001) and Raja et al. (2010) when computing the inertial correction to the stresslet in shear-dominated flows. Since the droplet lies entirely within the Stokes region, the Stokes flow field may be used to compute \mathbf{f}_i , and consequently the inertial terms involving \mathbf{f}_i in Eq. (4.16).

Based on this argument and Eqs. (3.10) and (4.10), one may re-write the forcing terms as,

$$\mathbf{f}_{i/o} = \mathbf{w}_r \cdot (\mathbb{U}_{i/o}^{(1)} + \boldsymbol{\delta}) \cdot \nabla \mathbb{U}_{i/o}^{(1)} \cdot \mathbf{w}_r, \quad (4.17)$$

and compute the last integrals on the right-hand side of Eqs. (4.3) and (4.16), yielding:

$$\oint_{\Gamma_p} \mathbf{r} \boldsymbol{\sigma}_o \cdot \mathbf{n} d\Gamma - \int_{\Omega_i} 2\mathbf{e}_i d\Omega \stackrel{i \neq j}{=} -\pi Re \frac{63\lambda^3 + 150\lambda^2 + 112\lambda + 28}{60(\lambda + 1)^3} \mathbf{w}_r \mathbf{w}_r, \quad (4.18)$$

$$\oint_{\Gamma_p} \mathbf{r} \cdot \boldsymbol{\sigma}_o \cdot \mathbf{n} d\Gamma = \pi Re \frac{3\lambda^2 + 6\lambda + 4}{12(\lambda + 1)^2} \mathbf{w}_r \cdot \mathbf{w}_r, \quad (4.19)$$

To obtain a formula for the whole first moment, we sum the deviatoric part of Eq. (4.18) with Eq. (4.19) times $\delta_{ij}/3$. It gives,

$$\begin{aligned} \oint_{\Gamma_p} \mathbf{r} \boldsymbol{\sigma}_o \cdot \mathbf{n} d\Gamma - \int_{\Omega_i} 2\mathbf{e}_i d\Omega &= -\pi Re \frac{63\lambda^3 + 150\lambda^2 + 112\lambda + 28}{60(\lambda + 1)^3} \mathbf{w}_r \mathbf{w}_r, \\ &+ \pi Re \frac{26\lambda^3 + 65\lambda^2 + 54\lambda + 16}{60(\lambda + 1)^3} (\mathbf{w}_r \cdot \mathbf{w}_r) \boldsymbol{\delta}. \end{aligned} \quad (4.20)$$

Additionally, using Eqs. (3.10) and (4.7) and similar arguments for the estimation of $\mathbf{f}_{i/o}$ one find:

$$\oint_{\Gamma_p} \mathbf{u}_i \mathbf{r} d\Gamma = \int_{\Omega_i} \mathbf{e}_i d\Omega = -\pi Re \frac{12\lambda^2 + 23\lambda + 10}{100(\lambda + 1)^3} [\mathbf{w}_r \mathbf{w}_r - \frac{1}{3} (\mathbf{w}_r \cdot \mathbf{w}_r) \boldsymbol{\delta}] \quad (4.21)$$

which may be used to compute the droplet deformation in that particular situation following the procedure of Fintzi and Pierson (2025).

4.2.3 Second moment of force

Now, let us turn our attention to the second moment of forces. Since \mathbf{w}_r is uniform and $\mathbf{b} = 0$, Eq. (4.4) reads

$$\begin{aligned} \frac{1}{2} \oint_{\Gamma_p} r_k r_j (\boldsymbol{\sigma}_o \cdot \mathbf{n})_i d\Gamma - 2 \int_{\Omega_i} r_k (\mathbf{e}_i)_{ji} d\Omega &\stackrel{i \neq j, k}{=} (\mathbf{w}_r)_l \oint_{\Gamma_p} (\mathbb{S}_o^{(3)})_{ijklm} n_m d\Gamma \\ &+ \zeta Re \int_{\Omega_i} ((\mathbb{U}_i^{(3)})_{ijkl} + \frac{1}{2} r_k r_j \delta_{il}) (\mathbf{f}_i)_l d\Omega + Re \int_{\Omega_o} (\mathbb{U}_o^{(3)})_{ijkl} (\mathbf{f}_o)_l d\Omega. \end{aligned} \quad (4.22)$$

This formula gives the second moment of forces (left-hand side of Eq. (4.22)) for a droplet translating in a uniform flow. As noted, previously we have factored out by $(\nabla \nabla \hat{\mathbf{U}})_{kji}$, to derive this formula, hence Eq. (4.22) is only valid when $i \neq j, k$. To obtain the traces of the second moment, i.e., K_{lkl} and K_{lk} , we use a procedure similar to the one used for Eq. (4.3) (see Section B.2). Indeed, based on the singularity solutions given by Eq. (3.13) we may show that,

$$\frac{1}{2} \oint_{\Gamma_p} \mathbf{n} \mathbf{n} \cdot \boldsymbol{\sigma}_o \cdot \mathbf{n} d\Gamma = -\frac{1}{2} \oint_{\Gamma_p} \boldsymbol{\sigma}_o \cdot \mathbf{n} d\Gamma + 3\mathbf{w}_r \int_{\Omega_i} d\Omega + \frac{Re}{2} \int_{\Omega_o} (\boldsymbol{\delta} + \mathbf{n} \mathbf{n}) r^{-1} \cdot \mathbf{f}_o d\Omega, \quad (4.23)$$

$$\frac{1}{2} \oint_{\Gamma_p} \mathbf{n} \mathbf{n} \cdot \boldsymbol{\sigma}_o \cdot \mathbf{n} d\Gamma - \oint_{\Gamma_p} 2\mathbf{r} \cdot \mathbf{e}_i d\Gamma = \frac{1}{6} \oint_{\Gamma_p} \boldsymbol{\sigma}_o \cdot \mathbf{n} d\Gamma + \frac{Re}{6} \int_{\Omega_o} (\boldsymbol{\delta} - 3\mathbf{n} \mathbf{n}) r^{-3} \cdot \mathbf{f}_o d\Omega. \quad (4.24)$$

It is interesting to note that the drag force term appear explicitly on the right-hand side of these expressions. Here, it should be understood that Eq. (4.23) corresponds to \mathbb{K}_{lkl} , while equation Eq. (4.24) corresponds to \mathbb{K}_{lk} .

Whether, it is Eqs. (4.22) to (4.24) the vectors $\mathbf{f}_{i/o}$ are still needed, and given by Eq. (4.10), with the approximation given by $\mathbf{u}_{i/o} = \mathbf{w}_r \cdot \mathbb{U}_{i/o}^{(1)}$ close from the test droplet, and $\mathbf{u}_o = \mathbf{f} \cdot \mathbb{U}^{(out)}$ in the Oseen region. Additionally, in stretched coordinates one find (Nadim and Stone, 1991),

$$\frac{1}{Re} (\mathbb{U}^{(3)})_{ijkl} = \pi \frac{\lambda}{(\lambda + 1)} (\tilde{\mathbb{G}})_{li} \delta_{jk} + O(Re), \quad (4.25)$$

at the leading order in Re . Hence, the last integrals on the right-hand side of Eqs. (4.22) to (4.24) will be evaluated using the same approach as for Eq. (4.8) and Eq. (4.16). Using the same symmetry arguments as in the two previous sections, we arrive at the conclusion that in Eqs. (4.22) to (4.24) all the internal contributions integrated over the volume of the test droplet vanish except the second term of Eq. (4.23). By making use of the same symmetry argument as in the drag force calculation, and of Eq. (4.25), we deduce that in Eqs. (4.22) and (4.23), only the far field contribution is relevant. The result of the integral presented in Eq. (4.14) is used to compute these two contributions. In the last integral on the right-hand side of Eq. (4.24), only the inner velocity field could in principle contribute, due to the rapid r^{-3} decay of the integrand. However, the contribution from the inner velocity field vanishes upon integration, since the final expression is odd in \mathbf{n} . Overall, the methodology for computing the integrals requires nothing beyond what has already been presented in the previous two subsections. This yields,

$$\frac{1}{2} \oint_{\Gamma_p} r_k r_j (\boldsymbol{\sigma}_o \cdot \mathbf{n})_i d\Gamma - 2 \int_{\Omega_i} r_k (\mathbf{e}_i)_{ji} d\Omega \stackrel{i \neq j, k}{=} \pi \frac{\lambda}{\lambda + 1} (\mathbf{w}_r)_i \delta_{jk} + Re \pi \frac{\lambda(2 + 3\lambda)}{8(\lambda + 1)^2} \delta_{jk} (\mathbf{w}_r)_i, \quad (4.26)$$

$$\frac{1}{2} \oint_{\Gamma_p} \mathbf{n} \mathbf{n} \cdot \boldsymbol{\sigma}_o \cdot \mathbf{n} d\Gamma = \pi \frac{\lambda + 2}{\lambda + 1} \mathbf{w}_r + Re \pi \frac{(2 + \lambda)(2 + 3\lambda)}{8(\lambda + 1)^2} \mathbf{w}_r, \quad (4.27)$$

$$\frac{1}{2} \oint_{\Gamma_p} \mathbf{n} \mathbf{n} \cdot \boldsymbol{\sigma}_o \cdot \mathbf{n} d\Gamma - \oint_{\Gamma_p} 2\mathbf{r} \cdot \mathbf{e}_i d\Gamma = \pi \frac{3\lambda + 2}{3(\lambda + 1)} \mathbf{w}_r + \pi \frac{(3\lambda + 2)^2}{24(\lambda + 1)^2} \mathbf{w}_r. \quad (4.28)$$

Combining all contributions and using Eq. (4.5) and Eq. (4.6) yields the expression for the complete second moment of the forces, namely,

$$\begin{aligned} \frac{1}{2} \oint_{\Gamma_p} r_k r_j (\boldsymbol{\sigma}_o \cdot \mathbf{n})_i d\Gamma - 2 \int_{\Omega_i} r_k (\mathbf{e}_i)_{ji} d\Omega &= \frac{\pi}{\lambda + 1} \left[\frac{2}{3} \delta_{ij} (\mathbf{w}_r)_k + \lambda \delta_{jk} (\mathbf{w}_r)_i \right] \\ &\quad + \frac{\pi Re(3\lambda + 2)}{8(\lambda + 1)^2} \left[\frac{2}{3} \delta_{ij} (\mathbf{w}_r)_k + \lambda \delta_{jk} (\mathbf{w}_r)_i \right]. \end{aligned} \quad (4.29)$$

One may note that the Stokes-flow contribution derived in [Zhang and Prosperetti \(1997\)](#); [Fintzi and Pierson \(2025\)](#) is recovered in the first line of Eq. (4.29).

4.3 Discussion

The formulas given by Eqs. (4.20) and (4.29) constitute the main results of the paper. One may note the absence of ζ in these expressions, indicating that the droplet density has no effect on the first and second moment at least for $Re \ll 1$ and $Ca \ll 1$. This arises because, upon direct calculation, the first integral on the right-hand side of Eq. (4.16) vanishes. Moreover, as shown previously, the inertial contributions integrated over the volume of the test droplet also vanish in the expressions for the second moment; consequently, the droplet density has no effect on the second moment. A similar observation was made by [Magnaude et al. \(2003\)](#), who showed that the inertial lift force acting on a droplet translating parallel to a wall does not depend on the droplet density. However, [Taylor and Acrivos \(1964\)](#) demonstrated that the density ratio enters the force balance through droplet deformation. Therefore, one may expect the density ratio to influence the force moments for a slightly deformed droplet.

5 Averaged zeroth, first, and second moments of forces

Before presenting the averaged system of equations (Eqs. (2.1) to (2.5)) in a (nearly) closed form, we first introduce the averaged and dimensional expressions of the force, first moment, and second moment of the forces. Indeed, the results derived in the previous sections still need to be converted back to dimensional form and integrated over all particle centre-of-mass velocities (\mathbf{w}) (Eq. (2.11)). Hence, below the vectors $\mathbf{w}_r, \mathbf{U}_p$ and \mathbf{U} refer to the dimensional velocity vectors.

First, note that all stresses appearing on the left-hand side of Eqs. (4.15), (4.20) and (4.29) were nondimensionalized using the stress scale $\mu_f U/a$, with lengths scaled by a . In addition, recall that the Reynolds number is defined as ($Re = U \rho_f a / \mu_f$). As a result, the viscous contributions in Eqs. (4.15) and (4.29) scale linearly with the relative velocity ($\mathbf{w}_r = \mathbf{U} - \mathbf{w}$). Therefore, upon averaging over all values of \mathbf{w} , one simply obtains:

$$\int_{\mathbb{R}^3} P[\mathbf{w}|\mathbf{x}, t] \mathbf{w}_r d\mathbf{w} = \mathbf{U} - \mathbf{U}_p = \mathbf{U}_r, \quad (5.1)$$

where we have introduced \mathbf{U}_r as the mean relative velocity between phases. In dimensional form the first moment of forces, given by Eq. (4.20), scale as $\mathbf{w}_r \mathbf{w}_r$. Hence, upon

averaging overall \mathbf{w} one obtain,

$$n_p[\mathbf{x}, t] \int_{\mathbb{R}^3} P[\mathbf{w}|\mathbf{x}, t] \mathbf{w}_r \mathbf{w}_r d\mathbf{w} = n_p \mathbf{U}_r \mathbf{U}_r + \langle \delta_p \mathbf{u}'_\alpha \mathbf{u}'_\alpha \rangle, \quad (5.2)$$

where we recall that $\langle \delta_p \mathbf{u}'_\alpha \mathbf{u}'_\alpha \rangle$ represents the variance of the droplet center-of-mass velocity, which is responsible for the momentum flux appearing in Eq. (2.4). We now turn our attention to the Oseen force and to the inertial contribution to the second moment of the force, given by Eqs. (4.15) and (4.29). In dimensional form, these expressions involve integrals of terms proportional to $|\mathbf{w}_r| \mathbf{w}_r$. Since $|\mathbf{w}_r|$ is a nonlinear (power-law) function of \mathbf{w}_r , its average cannot, for an arbitrary distribution ($P[\mathbf{w}|\mathbf{x}, t]$), be expressed solely in terms of the mean relative velocity (\mathbf{U}_r) and $\langle \delta_p \mathbf{u}'_\alpha \mathbf{u}'_\alpha \rangle$. Nevertheless, if we assume that \mathbf{w} remains close to \mathbf{U}_p , one may perform a Taylor expansion of \mathbf{w}_r about \mathbf{U}_r , leading to the approximation (see Section C)

$$n_p \int_{\mathbb{R}^3} |\mathbf{w}_r| (\mathbf{w}_r)_k P(\mathbf{w}) d\mathbf{w} = n_p |\mathbf{U}_r| (\mathbf{U}_r)_k + n_p (\mathbf{R}_p)_k + O(\langle \delta_p (\mathbf{u}'_\alpha)^{(3)} \rangle) \quad (5.3)$$

with $\mathbf{p} = \mathbf{U}_r |\mathbf{U}_r|^{-1}$ the unit vector in the direction of \mathbf{U}_r , and,

$$n_p (\mathbf{R}_p)_k = 1/2 \langle \delta_p \mathbf{u}'_\alpha \mathbf{u}'_\alpha \rangle_{ij} (\delta_{ij} p_k + 2p_j \delta_{ik} - p_i p_j p_k). \quad (5.4)$$

The error generated by this approximation scale as $O(\langle \delta_p (\mathbf{u}'_\alpha)^{(3)} \rangle)$, corresponding to the third-order moments of the distribution $P[\mathbf{w}|\mathbf{x}, t]$. Consequently, if $P[\mathbf{w}|\mathbf{x}, t]$ is a normal distribution this expression is exact, since the skewness and all higher-order moments vanish.

In summary, by averaging Eqs. (4.15), (4.20) and (4.29) over all \mathbf{w} , and using Eqs. (5.1) to (5.3), we obtain the ensemble-averaged zeroth, first, and second moments of the forces, which in dimensional form read,

$$\left\langle \delta_p \oint_{\Gamma_\alpha} \boldsymbol{\sigma}_f^* \cdot \mathbf{n} d\Gamma \right\rangle = \frac{\mu_f}{a^2} \frac{3(2+3\lambda)}{2(\lambda+1)} \phi \mathbf{U}_r + \frac{\rho_f}{a} \frac{3(2+3\lambda)^2}{16(\lambda+1)^2} \phi (|\mathbf{U}_r| \mathbf{U}_r + \mathbf{R}_p), \quad (5.5)$$

$$\begin{aligned} \left\langle \delta_p \oint_{\Gamma_\alpha} \mathbf{r} \boldsymbol{\sigma}_f^* \cdot \mathbf{n} d\Gamma \right\rangle - \left\langle \delta_p \int_{\Omega_\alpha} 2\mu_f \mathbf{e}_d^* d\Omega \right\rangle = \\ - \rho_f \frac{63\lambda^3 + 150\lambda^2 + 112\lambda + 28}{80(\lambda+1)^3} [\phi \mathbf{U}_r \mathbf{U}_r + v_p \langle \delta_p \mathbf{u}'_\alpha \mathbf{u}'_\alpha \rangle] \\ + \rho_f \frac{26\lambda^3 + 65\lambda^2 + 54\lambda + 16}{80(\lambda+1)^3} (\phi \mathbf{U}_r \cdot \mathbf{U}_r + v_p \langle \delta_p \mathbf{u}'_\alpha \cdot \mathbf{u}'_\alpha \rangle) \boldsymbol{\delta} \end{aligned} \quad (5.6)$$

$$\begin{aligned} \frac{1}{2} \left\langle \delta_p \oint_{\Gamma_\alpha} r_k r_j (\boldsymbol{\sigma}_o \cdot \mathbf{n})_{ij} d\Gamma \right\rangle - \left\langle \delta_p \int_{\Omega_\alpha} 2\mu_f r_k (\mathbf{e}_i)_{ji} d\Omega \right\rangle = \\ + \phi \mu_f \frac{3}{4(\lambda+1)} \left[\frac{2}{3} \delta_{ij} (\mathbf{U}_r)_k + \lambda \delta_{jk} (\mathbf{U}_r)_i \right] \\ + \phi \rho_f \frac{3(3\lambda+2)}{32(\lambda+1)^2} \left[\frac{2}{3} \delta_{ij} (|\mathbf{U}_r| \mathbf{U}_r + \mathbf{R}_p)_k + \lambda \delta_{jk} (|\mathbf{U}_r| \mathbf{U}_r + \mathbf{R}_p)_i \right], \end{aligned} \quad (5.7)$$

As discussed in Lhuillier (1996) and Fintzi and Pierson (2025, Eq. (5.35)), in the averaged momentum equation (Eq. (2.5)) the second moment of forces, noted \mathbb{K}_{ijk} here (Eq. (5.7)), appears as,

$$\begin{aligned} \mathbb{K}_{i(jk)} + \mathbb{K}_{j(ik)} - \mathbb{K}_{k(ij)} &= \phi \mu_f \frac{3\lambda}{4(\lambda+1)} [\delta_{ik}(\mathbf{U}_r)_j + \delta_{jk}(\mathbf{U}_r)_i] + \mu_f \phi \frac{2-3\lambda}{4(\lambda+1)} \delta_{ij}(\mathbf{U}_r)_k \\ &+ \phi a \rho_f \frac{3(3\lambda+2)\lambda}{32(\lambda+1)^2} [\delta_{ik}(\mathbf{U}_r|\mathbf{U}_r| + \mathbf{R}_p)_j + \delta_{jk}(\mathbf{U}_r|\mathbf{U}_r| + \mathbf{R}_p)_i] \\ &- \phi a \rho_f \frac{(3\lambda-2)(3\lambda+2)}{32(\lambda+1)^2} \delta_{ij}(\mathbf{U}_r|\mathbf{U}_r| + \mathbf{R}_p)_k, \end{aligned} \quad (5.8)$$

where the $\mathbb{K}_{i(jk)}$ represents the symmetric part of the tensor over the indices j and k , *i.e.* $\mathbb{K}_{i(jk)} = 1/2(\mathbb{K}_{ijk} + \mathbb{K}_{ikj})$, and so on for $\mathbb{K}_{j(ik)}$ and $\mathbb{K}_{k(ij)}$. Only the permutations of \mathbb{K} shown in Eq. (5.8) are physically relevant, since the tensor \mathbb{K} appears under the double divergence operator $\partial_k \partial_j$, in Eq. (2.5) (Lhuillier, 1996; Fintzi and Pierson, 2025). This transformation highlights that the associated effective stress is symmetric with respect to the pair of indices (i, j) .

It is also worth noting that, in potential flow, the inviscid first moment tensor reads (Biesheuvel and Van Wijngaarden, 1984; Zhang and Prosperetti, 1994),

$$a \left\langle \delta_p \oint_{\Gamma_\alpha} -p \mathbf{n} \mathbf{n} d\Gamma \right\rangle = -\rho_f \frac{9}{20} [\phi \mathbf{U}_r \mathbf{U}_r + v_p \langle \delta_p \mathbf{u}'_\alpha \mathbf{u}'_\alpha \rangle] + \rho_f \frac{2}{5} (\phi \mathbf{U}_r \cdot \mathbf{U}_r + v_p \langle \delta_p \mathbf{u}'_\alpha \cdot \mathbf{u}'_\alpha \rangle) \boldsymbol{\delta}$$

This formula is valid for a spherical bubble in the high-Reynolds-number limit. Taking the limit ($\lambda \rightarrow 0$) in Eq. (5.6) yields a coefficient of $-7/20$ for the deviatoric part and $1/5$ for the isotropic part. These values may be compared with the inviscid potential-flow coefficients, $-9/20$ and $2/5$, respectively. To the best of the authors knowledge, the second-order moment of the force has not been computed in the potential-flow regime. Nevertheless, based on the symmetry of the potential flow field generated by the steady motion of a particle, the inviscid steady contribution to the second moment is expected to vanish. There is, however, no reason for the viscous potential contribution to the second moment to be zero, although its explicit calculation lies beyond the scope of the present work.

6 Discussion and quasi-steady deformation

Although we consider linear and quadratic components of the flow in the averaged equation, we retain only inertial effects arising from uniform relative motion. Accordingly, we assume the scalings $a|\nabla \mathbf{U}| \approx a^2|\nabla \nabla \mathbf{U}| \ll U$ implying that inertial effects associated with shear or with the quadratic components of the velocity field can be neglected. Therefore, the results from the Stokes regime given in Fintzi and Pierson (2025) (see also Zhang and Prosperetti (1997)) can simply be added with the one given in the previous sections (Eqs. (5.5) to (5.8)) and yields,

$$\mathbf{F} = \phi \frac{\mu_f}{a^2} \frac{3(2+3\lambda)}{2(1+\lambda)} \mathbf{U}_{r,\text{Oseen}} + \phi \mu_f \frac{3\lambda}{4(\lambda+1)} \nabla^2 \mathbf{U} \quad (6.1)$$

$$\begin{aligned} \boldsymbol{\Sigma}_f^{\text{eff}} = & \mu_f \phi \frac{5\lambda+2}{2(\lambda+1)} \mathbf{E} \\ & - \mu_f \frac{3\lambda}{4(\lambda+1)} [\nabla(\phi \mathbf{U}_{r,\text{Oseen}}) + \nabla(\phi \mathbf{U}_{r,\text{Oseen}})^\dagger] + \mu_f \frac{3\lambda-2}{4(\lambda+1)} \nabla \cdot (\phi \mathbf{U}_{r,\text{Oseen}}) \boldsymbol{\delta} \\ & - \rho_f \frac{63\lambda^3 + 150\lambda^2 + 112\lambda + 28}{80(\lambda+1)^3} [\phi \mathbf{U}_r \mathbf{U}_r + v_p \langle \delta_p \mathbf{u}'_\alpha \mathbf{u}'_\alpha \rangle] \\ & + \rho_f \frac{26\lambda^3 + 65\lambda^2 + 54\lambda + 16}{80(\lambda+1)^3} (\phi \mathbf{U}_r \cdot \mathbf{U}_r + v_p \langle \delta_p \mathbf{u}'_\alpha \cdot \mathbf{u}'_\alpha \rangle) \boldsymbol{\delta} \\ & - \langle \chi_f \rho_f \mathbf{u}'_f \mathbf{u}'_f \rangle, \end{aligned} \quad (6.2)$$

$$\boldsymbol{\Sigma}_p^{\text{eff}} = - \rho_d v_p \langle \delta_p \mathbf{u}'_\alpha \mathbf{u}'_\alpha \rangle, \quad (6.3)$$

where we introduced the definition:

$$\mathbf{U}_{r,\text{Oseen}} = \mathbf{U}_r + \frac{\rho_f a}{\mu_f} \frac{2+3\lambda}{8(\lambda+1)} [\mathbf{U}_r |\mathbf{U}_r| + \mathbf{R}_p]. \quad (6.4)$$

The system of equations consisting of Eqs. (2.1) to (2.5) together with Eqs. (6.1) to (6.4) is fully closed, except for the velocity-variance terms $\langle \delta_p \mathbf{u}'_\alpha \mathbf{u}'_\alpha \rangle$ and $\langle \chi_f \mathbf{u}'_f \mathbf{u}'_f \rangle$. To determine these quantities, one may either solve transport equations for the variances, as commonly done in turbulence modeling (Pope, 2001) and kinetic theory (Rao et al., 2008), or introduce explicit closures that relate the variances to \mathbf{U}_r , λ , ϕ , and their gradients, and, when relevant, the problem boundaries. In the regime where only pseudo-turbulence is present, it is reasonable to expect that the functional form of such closures does not introduce new qualitative behaviors beyond those already contained in the effective stress tensor ($\boldsymbol{\Sigma}_f^{\text{eff}}$). Consequently, the discussion that follows remains qualitatively valid even after including these closures. Hints on their modeling is provided in Fintzi and Pierson (2025). In addition, closures for the velocity variances of both the continuous and dispersed phases in the Oseen regime can be found in Koch (1993).

Owing to the rigorous averaging procedure employed here, we have shown that the velocity variance of the dispersed phase appears explicitly in the expression for the force. To the best of our knowledge, this point has not been raised previously, although the inclusion of relative-velocity variance in drag-force models is common in two-phase flow modeling (Simonin, 1996). While the Oseen drag law is valid only over a limited range of Reynolds numbers (Chester et al., 1969), the present results highlight that, when an isolated-particle model is used within an averaged framework, it is necessary to also average over the center-of-mass velocity of the test particle. This procedure naturally introduces higher-order moments of the dispersed-phase velocity distribution. For instance, the various empirical closures available in the literature for isolated particles (Clift et al., 2005), when averaged over the particle center-of-mass velocity, would acquire additional contributions proportional to the velocity variance. The same remarks apply to the first and second moments of the force.

A second point worth discussing is the presence of a term proportional to $\rho_f \phi \mathbf{U}_r \mathbf{U}_r$ in the effective stress tensor. This term is clearly non-negligible in buoyant droplet

suspensions due to the strong relative motion between the phases. In particular, it may be of the same order of magnitude as the Newtonian viscous stress proportional to $\mu_f \phi \mathbf{E}$ when the Reynolds number associated with the relative motion is sufficiently large. However, these two contributions have very different physical effects. For example, in a vertical established flow with relative velocity only in the channel direction, the divergence of the inertial Stresslet tensor vanishes in the vertical momentum balance. However, the Stresslet may have an impact on the horizontal momentum balance which may in turn modify the radial distribution of ϕ , which may then eventually impact the vertical momentum balance.

In Eq. (6.2) we clearly see that the second moment of force contribution, at $O(Re)$, has exactly the same functional form as in the Stokes flow regime except that the relative velocity is $\mathbf{U}_{r,Oseen}$ as defined in Eq. (6.4), instead of \mathbf{U}_r in Stokes flow regime. This is an expected result as the Oseen outer solution basically increases “the uniform background flow velocity” seen by the droplet by that amount (i.e. by the second term of Eq. (6.4)). According to Eqs. (4.23) and (4.24) we know that the traces of the second moment is among other contribution exactly proportional to the Drag force on particles. The way we factorized Eq. (6.2) with $\mathbf{U}_{r,Oseen}$ seems to support this argument to the whole second moment tensor. Thus, for future engineering practices, one could use the Drag force coefficients available in the literature to extend this model of second moment of force to higher Re .

The inertial correction to the second moment of the force is proportional to the gradient of a term of the form $a\rho_f \phi \mathbf{U}_r |\mathbf{U}_r|$. Depending on the magnitudes of $\nabla\phi$ and $\nabla\mathbf{U}_r$ (or $\nabla|\mathbf{U}_r|$), this contribution may be of the same order of magnitude compared to the inertial contribution arising from the first moment. However, the scale-separation hypothesis implicitly used in this derivation assumes that these gradients vary over a characteristic length scale (L) that is much larger than the droplet radius. As a result, the inertial second moment contribution, are of order $O(a/L)$ relative to the inertial contribution of the first moment. Consequently, the inertial contribution of the second moment is probably negligible in practical models of suspension rheology.

Overall, the mixture momentum equation obtained by summing Eqs. (2.4) and (2.5) does not correspond to a Newtonian fluid. This non-Newtonian behaviour arises from the Stokes contribution of the second moment, the inertial contribution of the first moment, and, to a lesser extent, the inertial contribution of the second moment. In the averaged momentum equation of the continuous phase (Eq. (2.5)), it is the divergence of the stress tensor that governs the dynamics. Accordingly, the first moment contributes through the terms $\rho_f \mathbf{U}_r \mathbf{U}_r \cdot \nabla\phi$ and $\rho_f \phi \nabla \cdot (\mathbf{U}_r \mathbf{U}_r)$. Therefore, in situations where strong gradients of the volume fraction or pronounced spatial variations in \mathbf{U}_r are present-as is the case, for instance, in flows near a wall (Cox and Mason, 1971)-these stress contributions may play an important role. Although as discussed previously for the vertical channel flow their physical relevance needs to be carefully examined.

Acknowledgment

The authors thank H. Stone for sharing his unpublished work (Stone et al., 2001), which greatly inspired the present study. We also thank him for his comments on an earlier draft of this manuscript.

References

Batchelor, G. (1970). The stress system in a suspension of force-free particles. *Journal of Fluid Mechanics*, 41(3):545–570.

Biesheuvel, A. and Van Wijngaarden, L. (1984). Two-phase flow equations for a dilute dispersion of gas bubbles in liquid. *Journal of Fluid Mechanics*, 148:301–318.

Brenner, H. (1964). The stokes resistance of an arbitrary particle-iv arbitrary fields of flow. *Chemical Engineering Science*, 19(10):703–727.

Bulthuis, H., Prosperetti, A., and Sangani, A. (1995). Particle stress in disperse two-phase potential flow. *Journal of Fluid Mechanics*, 294:1–16.

Buyevich, Y. A. and Shchelchkova, I. (1979). Flow of dense suspensions. *Progress in Aerospace Sciences*, 18:121–150.

Caflisch, R. E. and Luke, J. H. (1985). Variance in the sedimentation speed of a suspension. *Physics of Fluids*, 28(3):759–760.

Candelier, F., Mehaddi, R., Mehlig, B., and Magnaudet, J. (2023). Second-order inertial forces and torques on a sphere in a viscous steady linear flow. *Journal of Fluid Mechanics*, 954:A25.

Candelier, F. and Mehlig, B. (2016). Settling of an asymmetric dumbbell in a quiescent fluid. *Journal of Fluid Mechanics*, 802:174–185.

Chester, W., Breach, D., and Proudman, I. (1969). On the flow past a sphere at low reynolds number. *Journal of Fluid Mechanics*, 37(4):751–760.

Clift, R., Grace, J. R., and Weber, M. E. (2005). Bubbles, drops, and particles.

Cox, R. and Mason, S. (1971). Suspended particles in fluid flow through tubes. *Annual Review of Fluid Mechanics*, 3(1):291–316.

Dabade, V., Marath, N. K., and Subramanian, G. (2015). Effects of inertia and viscoelasticity on sedimenting anisotropic particles. *Journal of Fluid Mechanics*, 778:133–188.

Drew, D. A. (1983). Mathematical modeling of two-phase flow. *Annual review of fluid mechanics*, 15(1):261–291.

Einstein, A. (1905). *Eine neue bestimmung der moleküldimensionen*. PhD thesis, ETH Zurich.

Fintzi, N. (2025). *Statistical modeling of disperse two-phase flows : application to buoyancy-driven droplets suspensions*. PhD thesis, Sorbonne Universite.

Fintzi, N. and Pierson, J.-L. (2025). Averaged equations for disperse two-phase flow with interfacial properties and their closures for dilute suspension of droplets. *International Journal of Multiphase Flow*, page 105424.

Gatignol, R. (1983). The faxén formulae for a rigid particle in an unsteady non-uniform stokes flow.

Gatignol, R. (2023). *Thermomécanique des milieux continus*. Éditions Cépaduès.

Hadamard, J. (1911). Mouvement permanent lent d'une sphere liquide et visqueuse dans un liquide visqueux. (*No Title*), 152:1735.

Hetsroni, G. and Haber, S. (1970). The flow in and around a droplet or bubble submerged in an unbound arbitrary velocity field. *Rheologica Acta*, 9(4):488–496.

Hinch, E. (1977). An averaged-equation approach to particle interactions in a fluid suspension. *Journal of Fluid Mechanics*, 83(4):695–720.

Jackson, R. (1997). Locally averaged equations of motion for a mixture of identical spherical particles and a newtonian fluid. *Chemical Engineering Science*, 52(15):2457–2469.

Kantarci, N., Borak, F., and Ulgen, K. O. (2005). Bubble column reactors. *Process biochemistry*, 40(7):2263–2283.

Kaplun, S. and Lagerstrom, P. (1957). Asymptotic expansions of navier-stokes solutions for small reynolds numbers. *Journal of Mathematics and Mechanics*, pages 585–593.

Kim, S. and Karrila, S. J. (2013). *Microhydrodynamics: principles and selected applications*. Courier Corporation.

Koch, D. L. (1993). Hydrodynamic diffusion in dilute sedimenting suspensions at moderate reynolds numbers. *Physics of Fluids A: Fluid Dynamics*, 5(5):1141–1155.

Leal, L. (1980). Particle motions in a viscous fluid. *Annual Review of Fluid Mechanics*, 12:435–476.

Leal, L. G. (2007). *Advanced transport phenomena: fluid mechanics and convective transport processes*, volume 7. Cambridge University Press.

Levich, V. G. (1962). *Physicochemical hydrodynamics*. Prentice-Hall.

Lhuillier, D. (1992). Ensemble averaging in slightly non-uniform suspensions. *European journal of mechanics. B, Fluids*, 11(6):649–661.

Lhuillier, D. (1996). Contribution of the particulate phase to the overall stress of a suspension. *Comptes Rendus de l'Academie des Sciences-Serie IIb-Mecanique Physique Chimie Astronomie*, 323(1):3–8.

Lin, C.-J., Peery, J. H., and Schowalter, W. (1970). Simple shear flow round a rigid sphere: inertial effects and suspension rheology. *Journal of Fluid Mechanics*, 44(1):1–17.

Lovalenti, P. M. and Brady, J. F. (1993). The force on a bubble, drop, or particle in arbitrary time-dependent motion at small reynolds number. *Physics of Fluids A: Fluid Dynamics*, 5(9):2104–2116.

Magnaude, J., Takagi, S., and Legendre, D. (2003). Drag, deformation and lateral migration of a buoyant drop moving near a wall. *Journal of Fluid Mechanics*, 476:115–157.

Masoud, H. and Stone, H. A. (2019). The reciprocal theorem in fluid dynamics and transport phenomena. *Journal of Fluid Mechanics*, 879:P1.

Maxey, M. R. and Riley, J. J. (1983). Equation of motion for a small rigid sphere in a nonuniform flow. *The Physics of Fluids*, 26(4):883–889.

Nadim, A. and Stone, H. A. (1991). The motion of small particles and droplets in quadratic flows. *Studies in Applied Mathematics*, 85(1):53–73.

Nguyen, A. and Schulze, H. J. (2003). *Colloidal science of flotation*. CRC press.

Pope, S. B. (2001). Turbulent flows. *Measurement Science and Technology*, 12(11):2020–2021.

Pozrikidis, C. (2011). *Introduction to theoretical and computational fluid dynamics*. Oxford university press.

Pozrikidis, C. et al. (1992). *Boundary integral and singularity methods for linearized viscous flow*. Cambridge university press.

Proudman, I. and Pearson, J. (1957). Expansions at small reynolds numbers for the flow past a sphere and a circular cylinder. *Journal of Fluid Mechanics*, 2(3):237–262.

Raja, R. V., Subramanian, G., and Koch, D. L. (2010). Inertial effects on the rheology of a dilute emulsion. *Journal of Fluid Mechanics*, 646:255–296.

Rao, K. K., Nott, P. R., and Sundaresan, S. (2008). *An introduction to granular flow*, volume 490. Cambridge University Press Cambridge.

Rybczynski, W. (1911). Über die fortschreitende bewegung einer flüssigen kugel in einem zahlen medium. *Bull. Acad. Sci. Cracovie A*, 1:40–46.

Ryskin, G. and Rallison, J. (1980). The extensional viscosity of a dilute suspension of spherical particles at intermediate microscale reynolds numbers. *Journal of Fluid Mechanics*, 99(3):513–529.

Sangani, A. S. and Didwania, A. (1993). Dispersed-phase stress tensor in flows of bubbly liquids at large reynolds numbers. *Journal of Fluid Mechanics*, 248:27–54.

Simonin, O. (1996). Continuum modelling of dispersed two-phase flows. *Lecture series-Von Karman Institute for fluid dynamics*, 2:K1–K47.

Stone, H., Brady, J., and Lovalenti, P. (2001). Inertial effects on the rheology of suspensions and on the motion of individual particles. *preprint*.

Taylor, G. I. (1932). The viscosity of a fluid containing small drops of another fluid. *Proceedings of the Royal Society of London. Series A, Containing papers of a mathematical and physical character*, 138(834):41–48.

Taylor, T. and Acrivos, A. (1964). On the deformation and drag of a falling viscous drop at low reynolds number. *Journal of Fluid Mechanics*, 18(3):466–476.

Wallis, G. B. (2020). *One-dimensional two-phase flow*. Courier Dover Publications.

Weatherley, L. R. (2020). *Intensification of Liquid–Liquid Processes*. Cambridge University Press.

Zhang, D. and Prosperetti, A. (1994). Ensemble phase-averaged equations for bubbly flows. *Physics of Fluids*, 6(9):2956–2970.

Zhang, D. and Prosperetti, A. (1997). Momentum and energy equations for disperse two-phase flows and their closure for dilute suspensions. *International Journal of Multiphase Flow*, 23(3):425–453.

Zhou, G. and Prosperetti, A. (2020). Lamb solution and the stress moments for a sphere in stokes flow. *European Journal of Mechanics-B/Fluids*, 79:270–282.

A Points source, point force, and derivatives

In this appendix we demonstrate how to obtain the solution of a point source, point forces, and higher order derivatives of these flows. First, we recall the useful relation,

$$\delta(\mathbf{x}) = -\frac{1}{4\pi} \nabla^2(1/r) = -\frac{1}{8\pi} \nabla^4 r. \quad (\text{A.1})$$

The first equality only holds in the sense of generalized functions, the second equality can be obtained directly by differentiation of r . These relations are used several times in the demonstration below.

Point sources solutions : We start by the points source solutions, which obey the non-homogeneous Stokes equations:

$$\nabla \cdot \mathbf{u} = 0 \quad \nabla^2 \mathbf{u} = \nabla p + (\mathbf{Q}^{(n)} \odot \nabla^{(n)}) \nabla \delta(\mathbf{r}) \quad (\text{A.2})$$

Taking the divergence of the momentum equation gives,

$$\nabla^2 p = \frac{1}{4\pi} \nabla^{(n)} \nabla^2 \nabla^2(1/r) \odot \mathbf{Q}^{(n)} \iff p = \frac{1}{4\pi} \nabla^{(n)} \nabla^2(1/r) \odot \mathbf{Q}^{(n)} = 0 \quad (\text{A.3})$$

Hence, the momentum equation reads,

$$\nabla^2 \mathbf{u} = -\frac{1}{4\pi} \nabla^{(n+1)} \nabla^2(1/r) \odot \mathbf{Q}^{(n)} \iff \mathbf{u} = -\frac{1}{4\pi} \nabla^{(n+1)}(1/r) \odot \mathbf{Q}^{(n)} \quad (\text{A.4})$$

Because $\nabla \mathbf{u}$ is already symmetric and $p = 0$ we have,

$$\boldsymbol{\sigma} = 2\nabla \mathbf{u} = -\frac{1}{4\pi} 2\nabla^{(n+2)}(1/r) \odot \mathbf{Q}^{(n)}. \quad (\text{A.5})$$

Point force solutions : We seek a solution for,

$$\nabla \cdot \mathbf{u} = 0 \quad \nabla^2 \mathbf{u} = \nabla p + (\mathbf{R}^{(n+1)} \odot \nabla^{(n)}) \delta(\mathbf{r}) \quad (\text{A.6})$$

where $\mathbf{R}^{(n+1)}$ is an arbitrary $n+1$ order tensor. Taking the divergence of the momentum equation yields,

$$p = -\nabla^{(n+1)} \delta(\mathbf{r}) \odot \mathbf{R}^{(n+1)} = \frac{1}{4\pi} \nabla^{(n+1)}(1/r) \odot \mathbf{R}^{(n+1)} \quad (\text{A.7})$$

Hence, the momentum equation can be re-written,

$$\nabla^2 \mathbf{u} = \frac{1}{4\pi} \nabla^{(n)} [\nabla^{(2)} - \boldsymbol{\delta} \nabla^2] (1/r) \odot \mathbf{R}^{(n+1)} \quad (\text{A.8})$$

Using the second equality of Eq. (A.1) we directly deduce the solution of Eq. (A.8) as,

$$\mathbf{u} = \frac{1}{8\pi} \nabla^{(n)} [\nabla^{(2)} - \boldsymbol{\delta} \nabla^2] r \odot \mathbf{R}^{(n+1)}. \quad (\text{A.9})$$

The stress tensor then reads,

$$\boldsymbol{\sigma} = -p\boldsymbol{\delta} + \nabla \mathbf{u} + \nabla \mathbf{u}^\dagger = \frac{1}{8\pi} \nabla^{(n)} [2\nabla^{(3)} - (\nabla \boldsymbol{\delta} + \nabla \boldsymbol{\delta}^\dagger + \boldsymbol{\delta} \nabla) \nabla^2] r \odot \mathbf{R}^{(n+1)}. \quad (\text{A.10})$$

Taking $n = 0$ one recover the free space Green function of Stokes flows (Pozrikidis, 2011).

B Reciprocal relation for the second moment of force

B.1 Decomposition of a third-order tensor into a traceless tensor and isotopic contributions

The decomposition of \mathbb{K}_{ijk} into a deviatoric part and isotopic part, on only two indices is not a trivial task. Following the strategy of Nadim and Stone (1991) we consider an arbitrary third order tensor, \mathbb{K}_{ijk} , that represents the second moment of hydrodynamic forces. We assume that \mathbb{K} can be decomposed into the sum

$$\mathbb{K}_{ijk} = \mathbb{G}_{ijk} + (\mathbf{v}^1)_k \delta_{ij} + (\mathbf{v}^2)_j \delta_{ik}, \quad (\text{B.1})$$

where \mathbf{v}^1 and \mathbf{v}^2 are undetermined vectors, and \mathbb{G} is defined as the traceless part of \mathbb{K} under contractions over the index pairs ij and ik . As a result, \mathbf{v}^1 and \mathbf{v}^2 represent the isotropic parts of \mathbb{K} associated with the index pairs ij and ik , respectively. To express $\mathbf{v}^{1,2}$ in terms of the components of \mathbb{K} , we successively take the trace of Eq. Eq. (B.1) over ij and ik , which yields the following system of equations

$$\mathbb{K}_{llk} - 3(\mathbf{v}^1)_i - (\mathbf{v}^2)_i = 0, \quad (\text{B.2})$$

$$\mathbb{K}_{lil} - (\mathbf{v}^1)_i - 3(\mathbf{v}^2)_i = 0, \quad (\text{B.3})$$

$$(\text{B.4})$$

From which we deduce that,

$$(\mathbf{v}^1) = -\frac{1}{8}\mathbb{K}_{ljl} + \frac{3}{8}\mathbb{K}_{llj}, \quad (\text{B.5})$$

$$(\mathbf{v}^2) = \frac{3}{8}\mathbb{K}_{lkl} - \frac{1}{8}\mathbb{K}_{llk}. \quad (\text{B.6})$$

Finally, we can define the traceless part of \mathbb{K} (on only two pairs of indices), as

$$\mathbb{G}_{ijk} = \mathbb{K}_{ijk} - \left(\frac{3}{8}\right)\mathbb{K}_{ljl}\delta_{ik} - \left(\frac{3}{8}\right)\mathbb{K}_{llk}\delta_{ij} + \left(\frac{1}{8}\right)\mathbb{K}_{lkl}\delta_{ij} + \left(\frac{1}{8}\right)\mathbb{K}_{llj}\delta_{ik} \quad (\text{B.7})$$

Therefore, the formulas derived for the second moment in [Eq. \(4.4\)](#) provide only the tensor \mathbb{G}_{ijk} as defined in [Eq. \(B.7\)](#), and not the complete second-moment tensor \mathbb{K}_{ijk} . To recover the full second moment, expressions for \mathbf{v}^1 and \mathbf{v}^2 are still required. These vectors are entirely determined by \mathbb{K}_{lkl} and \mathbb{K}_{llk} , that is, by the traces of the second-moment tensor \mathbb{K}_{ijk} over the index pairs ik and ij , respectively.

B.2 Reciprocal theorem for the trace of the second moment

Formulas for $\mathbb{K}_{ijk}\delta_{ik}$ and $\mathbb{K}_{ijk}\delta_{ij}$, can be obtained using the point source dipole solution ([Eq. \(A.4\)](#) with $n = 1$) or the point force solution ([Eq. \(A.9\)](#) with $n = 0$). We start with [Eq. \(3.17\)](#) integrated on the exterior of the droplet:

$$-\oint_{\Gamma_p} \hat{\mathbf{u}}_o \cdot \boldsymbol{\sigma}_o \cdot \mathbf{n} d\Gamma = -\oint_{\Gamma_p} \mathbf{u}_o \cdot \hat{\boldsymbol{\sigma}}_o \cdot \mathbf{n} d\Gamma + \text{Re} \int_{\Omega_o} \hat{\mathbf{u}}_o \cdot \mathbf{f}_o d\Omega. \quad (\text{B.8})$$

Then we consider the test solutions given by [Eq. \(A.4\)](#) with $n = 1$, and [Eq. \(A.9\)](#) with $n = 0$, which read

$$\mathbf{u} = \frac{-1}{8\pi r}(\boldsymbol{\delta} + \mathbf{n}\mathbf{n}), \quad \boldsymbol{\sigma} \cdot \mathbf{n} = \frac{6}{8\pi r^{-2}}\mathbf{n}\mathbf{n}, \quad (\text{B.9})$$

$$\mathbf{u} = \frac{-1}{4\pi r^3}(3\mathbf{n}\mathbf{n} - \boldsymbol{\delta}), \quad \boldsymbol{\sigma} \cdot \mathbf{n} = \frac{-6}{4\pi r^4}(\boldsymbol{\delta} - 3\mathbf{n}\mathbf{n}), \quad (\text{B.10})$$

respectively. Inserting [Eq. \(B.9\)](#) and [Eq. \(B.10\)](#) in [Eq. \(B.8\)](#), we get

$$\oint_{\Gamma_p} (\boldsymbol{\delta} + \mathbf{n}\mathbf{n}) \cdot \boldsymbol{\sigma}_o \cdot \mathbf{n} d\Gamma = -6 \oint_{\Gamma_p} \mathbf{u}_o \cdot \mathbf{n} d\Gamma + \text{Re} \int_{\Omega_o} (\boldsymbol{\delta} + \mathbf{n}\mathbf{n}) r^{-1} \cdot \mathbf{f}_o d\Omega, \quad (\text{B.11})$$

$$\oint_{\Gamma_p} (3\mathbf{n}\mathbf{n} - \boldsymbol{\delta}) \cdot \boldsymbol{\sigma}_o \cdot \mathbf{n} d\Gamma = 6 \oint_{\Gamma_p} \mathbf{u}_o \cdot (\boldsymbol{\delta} - 3\mathbf{n}\mathbf{n}) d\Gamma + \text{Re} \int_{\Omega_o} (\boldsymbol{\delta} - 3\mathbf{n}\mathbf{n}) r^{-3} \cdot \mathbf{f}_o d\Omega, \quad (\text{B.12})$$

respectively. Using the two important identities:

$$\oint_{\Gamma_p} \mathbf{u}_o \cdot \mathbf{n} d\Gamma = \int_{\Omega_i} \nabla \cdot (\mathbf{u}_o \mathbf{n}) d\Omega = \int_{\Omega_i} \mathbf{u}_i d\Omega = -\mathbf{w}_r \int_{\Omega_i} d\Omega, \quad (\text{B.13})$$

and,

$$\begin{aligned}
\oint_{\Gamma_p} \mathbf{u}_o \cdot (\boldsymbol{\delta} - 3\mathbf{n}\mathbf{n}) d\Gamma &= -3 \oint_{\Gamma_p} \mathbf{u}_o \cdot \mathbf{n} d\Gamma + \oint_{\Gamma_p} \mathbf{u}_o \mathbf{n} \cdot \mathbf{n} d\Gamma \\
&= \oint_{\Gamma_p} \mathbf{u}_o \cdot \mathbf{n} d\Gamma + \oint_{\Gamma_p} \mathbf{u}_o \mathbf{n} \cdot \mathbf{n} d\Gamma - 4 \oint_{\Gamma_p} \mathbf{u}_o \cdot \mathbf{n} d\Gamma \\
&= \int_{\Omega_i} \nabla(\mathbf{u}_i \cdot \mathbf{r}) d\Omega + \int_{\Omega_i} \nabla \cdot (\mathbf{n} \mathbf{u}_i) d\Omega - 4 \int_{\Omega_i} \nabla \cdot (\mathbf{u}_i \mathbf{n}) d\Omega \\
&= \int_{\Omega_i} \nabla \mathbf{u}_i \cdot \mathbf{r} d\Omega + \int_{\Omega_i} \mathbf{u}_i d\Omega + 3 \int_{\Omega_i} \mathbf{u}_i d\Omega + \int_{\Omega_i} \mathbf{r} \cdot \nabla \mathbf{u}_i d\Omega - 4 \int_{\Omega_i} \mathbf{u}_i d\Omega \\
&= \int_{\Omega_i} \nabla \mathbf{u}_i \cdot \mathbf{r} d\Omega + \int_{\Omega_i} \mathbf{r} \cdot \nabla \mathbf{u}_i d\Omega \\
&= \int_{\Omega_i} 2\mathbf{r} \cdot \mathbf{e}_i d\Omega,
\end{aligned}$$

we may reformulate Eqs. (B.11) and (B.12) as,

$$\frac{1}{2} \oint_{\Gamma_p} \mathbf{n} \mathbf{n} \cdot \boldsymbol{\sigma}_o \cdot \mathbf{n} d\Gamma = -\frac{1}{2} \oint_{\Gamma_p} \boldsymbol{\sigma}_o \cdot \mathbf{n} d\Gamma + 3\mathbf{w}_r \int_{\Omega_i} d\Omega + \frac{Re}{2} \int_{\Omega_o} (\boldsymbol{\delta} + \mathbf{n} \mathbf{n}) r^{-1} \cdot \mathbf{f}_o d\Omega \quad (\text{B.14})$$

$$\frac{1}{2} \oint_{\Gamma_p} \mathbf{n} \mathbf{n} \cdot \boldsymbol{\sigma}_o \cdot \mathbf{n} d\Gamma - \oint_{\Gamma_p} 2\mathbf{r} \cdot \mathbf{e}_i d\Gamma = \frac{1}{6} \oint_{\Gamma_p} \boldsymbol{\sigma}_o \cdot \mathbf{n} d\Gamma + \frac{Re}{6} \int_{\Omega_o} (\boldsymbol{\delta} - 3\mathbf{n} \mathbf{n}) r^{-3} \cdot \mathbf{f}_o d\Omega. \quad (\text{B.15})$$

The first term on the right-hand side of Eqs. (B.14) and (B.15) is the drag forces acting upon the test droplet which can be obtained using its own reciprocal relation (Eq. (4.1)).

To conclude, we have derived Eq. (4.4) and we explained above that if, \mathbb{K}_{ijk} where the whole second moment of forces, then Eq. (4.4) would represent the tensor \mathbb{G}_{ijk} in the decomposition:

$$\mathbb{K}_{ijk} = \mathbb{G}_{ijk} + \frac{1}{8} (3\mathbb{K}_{ljl} - \mathbb{K}_{llj}) \delta_{ik} + \frac{1}{8} (3\mathbb{K}_{llk} - \mathbb{K}_{lkl}) \delta_{ij} \quad (\text{B.16})$$

Hence, to obtain the total second moment of forces, one must then add the traces \mathbb{K}_{llj} and \mathbb{K}_{ljl} to \mathbb{G}_{ijk} . In the previous subsection, we derived a formula for $\mathbb{K}_{ijk} \delta_{ij}$ which is given by Eq. (B.14), and a second one for $\mathbb{K}_{ijk} \delta_{ij}$ (Eq. (B.15)). Therefore, combining Eqs. (B.14), (B.15) and (4.4) following the decomposition given by Eq. (B.16), one directly obtains a formula for the complete second moment of forces.

C Average of the inertial correction

In this appendix, we provide a justification for Eq. (5.3). We begin by writing,

$$n_p[\mathbf{x}, t] \int_{\mathbb{R}^3} |\mathbf{w}_r| \mathbf{w}_r P(\mathbf{w}) d\mathbf{w}_r = n_p |\mathbf{U}_r| \mathbf{U}_r + n_p \int_{\mathbb{R}^3} (|\mathbf{w}_r| - |\mathbf{U}_r|) \mathbf{w}_r P(\mathbf{w}) d\mathbf{w}_r, \quad (\text{C.1})$$

and focus on the second term on the right-hand side of this equation. Provided that the deviation of \mathbf{w} around the mean velocity \mathbf{U}_p is small, one can use a Taylor expansion of the function $|\mathbf{w}_r|$ around $|\mathbf{U}_r|$, and write,

$$|\mathbf{w}_r| = |\mathbf{U}_r| + (\mathbf{w}_r - \mathbf{U}_r) \cdot \frac{\partial |\mathbf{w}_r|}{\partial \mathbf{w}_r} \bigg|_{\mathbf{w}_r=\mathbf{U}_r} + \frac{1}{2} (\mathbf{w}_r - \mathbf{U}_r) (\mathbf{w}_r - \mathbf{U}_r) : \frac{\partial |\mathbf{w}_r|}{\partial \mathbf{w}_r \partial \mathbf{w}_r} \bigg|_{\mathbf{w}_r=\mathbf{U}_r} + \dots \quad (\text{C.2})$$

Using the following identities,

$$\nabla |\mathbf{x}| = \mathbf{x} |\mathbf{x}|^{-1}, \quad (\text{C.3})$$

$$\nabla \nabla |\mathbf{x}| = \boldsymbol{\delta} |\mathbf{x}|^{-1} - \mathbf{x} \mathbf{x} |\mathbf{x}|^{-3}, \quad (\text{C.4})$$

yields,

$$|\mathbf{w}_r| - |\mathbf{U}_r| = (\mathbf{w}_r - \mathbf{U}_r) \cdot \mathbf{U}_r |\mathbf{U}_r|^{-1} + \frac{1}{2} (\mathbf{w}_r - \mathbf{U}_r) (\mathbf{w}_r - \mathbf{U}_r) : (\boldsymbol{\delta} |\mathbf{U}_r|^{-1} - \mathbf{U}_r \mathbf{U}_r |\mathbf{U}_r|^{-3}). \quad (\text{C.5})$$

Inserting this expression into Eq. (C.1), and integrating overall \mathbf{w} , while noting that $\mathbf{w}_r - \mathbf{U}_r = -\mathbf{w} + \mathbf{U}_p = -\mathbf{w}'$ is the fluctuation of the test droplet centre of mass velocity around \mathbf{U}_p , gives:

$$\begin{aligned} n_p \int_{\mathbb{R}^3} (|\mathbf{w}_r| - |\mathbf{U}_r|) \mathbf{w}_r P(\mathbf{w}) d\mathbf{w} \\ = n_p \int_{\mathbb{R}^3} [-\mathbf{w}' \cdot \mathbf{U}_r |\mathbf{U}_r|^{-1} + \frac{1}{2} \mathbf{w}' \mathbf{w}' : (\boldsymbol{\delta} |\mathbf{U}_r|^{-1} - \mathbf{U}_r \mathbf{U}_r |\mathbf{U}_r|^{-3})] \mathbf{U}_r P(\mathbf{w}) d\mathbf{w} \\ + n_p \int_{\mathbb{R}^3} [+ \mathbf{w}' \mathbf{w}' \cdot \mathbf{U}_r |\mathbf{U}_r|^{-1} - \frac{1}{2} \mathbf{w}' \mathbf{w}' \mathbf{w}' : (\boldsymbol{\delta} |\mathbf{U}_r|^{-1} - \mathbf{U}_r \mathbf{U}_r |\mathbf{U}_r|^{-3})] P(\mathbf{w}) d\mathbf{w}. \end{aligned}$$

Finally, by using the relation,

$$n_p \int_{\mathbb{R}^3} \mathbf{w}' \mathbf{w}' P(\mathbf{w}) d\mathbf{w} = \langle \delta_p \mathbf{u}'_\alpha \mathbf{u}'_\alpha \rangle,$$

and neglecting the triple covariance terms, we get,

$$\begin{aligned} n_p \int_{\mathbb{R}^3} |\mathbf{w}_r| (\mathbf{w}_r)_k P(\mathbf{w}) d\mathbf{w} \\ = n_p |\mathbf{U}_r| (\mathbf{U}_r)_k + \frac{1}{2} \langle \delta_p \mathbf{u}'_\alpha \mathbf{u}'_\alpha \rangle_{ij} (\delta_{ij} p_k + 2p_j \delta_{ik} - p_i p_j p_k) + O(\langle \delta_p (\mathbf{u}'_\alpha)^{(3)} \rangle), \quad (\text{C.6}) \end{aligned}$$

with $\mathbf{p} = \mathbf{U}_r |\mathbf{U}_r|^{-1}$ which proves Eq. (5.3).